Assessment of Radiation Streaming Through ARIES-CS He-Access Pipes using Two- and Three-Dimensional Analyses

A. Ibrahim, D.L. Henderson, L.A. El-Guebaly,
P.P.H. Wilson, M.E. Sawan

December 2007

UWFDM-1331

FUSION TECHNOLOGY INSTITUTE

UNIVERSITY OF WISCONSIN

MADISON WISCONSIN

Assessment of Radiation Streaming Through ARIES-CS He-Access Pipes using Two- and Three-Dimensional Analyses

A. Ibrahim, D.L. Henderson, L.A. El-Guebaly,
P.P.H. Wilson, M.E. Sawan

Fusion Technology Institute
University of Wisconsin
1500 Engineering Drive
Madison, WI 53706

http://fti.neep.wisc.edu

December 2007

UWFDM-1331

Abstract

Neutron streaming through penetrations compromises the shielding performance of fusion devices. To characterize the problem, the effects of neutron streaming through the divertor He-access pipe on the peaking of radiation-induced damage across the ARIES-CS power plant components were compared to the nominal values for the different components. The results show that due to streaming the damage exceeded the limits near the pipe for the manifolds, vacuum vessel, and magnet. Certain precautions should be taken that include changing the pipe design and orientation, avoiding rewelding the manifolds and vacuum vessel near the pipe, and/or relocating the magnet away from the pipe. This problem also provided a good test for both the deterministic and the Monte Carlo approaches. The analysis demonstrated the applicability of the deterministic transport codes, DANTSYS and Attila, to perform 2- and 3-D nuclear analyses of complex fusion systems and in particular the problem of radiation streaming. The analyses likewise showed that Attila cannot be used as a black box. Thought must be given to the generation of a workable CAD model using experiences gained from discrete ordinates deterministic codes before importing it into Attila. Negative fluxes in Attila results and discontinuities were noticed near the interface of the pipe and surrounding components. Some results obtained by Attila were compared to the University of Wisconsin newly developed CAD-based Monte Carlo code, DAG-MCNPX. The results compared well with the results of the Attila code being slightly lower than those from the DAG-MCNPX code, particularly near the end of the 2.7 m pipe.

Introduction

The ARIES Compact Stellarator (ARIES-CS) fusion power plant depicted in Fig. 1 is a geometrically complex fusion device that requires a detailed three-dimensional (3-D) model to assess the neutronics performance of the critical structures in the device. Generally, stellarators promise disruption-free operation with reduced recirculating power due to the absence of current-drive requirements. The compactness of ARIES-CS mandates that all components provide a shielding function [1]. Besides breeding tritium, the blanket protects the shield for the plant life (40 full power years). Along with the blanket, the shield is designed to protect the welds of the manifold and the vacuum vessel (VV). All four components help protect the superconducting magnet that operates at 4 K. The fusion power of the ARIES-CS is ~2400 MW, the average neutron wall loading (NWL) is 2.6 MW/m^2, and the net electric power is 1000 MW_e. All materials were carefully chosen to enhance the shielding performance and minimize the long-term environmental impact [1].

Penetrations are necessary for vacuum pumping, coolant supply lines, plasma control, and maintenance ports. Such penetrations jeopardize the effectiveness of the shield as neutron streaming through these penetrations enhances the damage near the interfaces of the shield, manifolds, VV, and magnet components. The most serious streaming issues are related to the large divertor He-access pipe. Of specific interest are the displacements per atom (dpa) and He production at the ferritic steel structure of the shield, manifolds, VV and pipe wall, the fast neutron fluence at the magnet, and the flux level behind the magnet. If the damage level in the structure is too high, these components will have to be replaced in order to maintain the integrity of the machine. The He production rate level should not exceed 1 appm at the manifolds and VV to be able to reweld these components during operation where cutting/rewelding is necessary to maintain the replaceable components (divertor and blanket). In addition, the displacement per atom should not exceed 200 dpa at the shield at any time during the expected 40 full power years (FPY) plant lifetime. Furthermore, the fast neutron fluence to the Nb_3Sn superconductor of the magnet should remain below 10^{19} n/cm^2 @ 40 FPY, the neutron flux outside the magnet should not be excessive to protect the externals, and the atomic displacement level should not exceed 10 dpa at the outer screws (that adjust the divertor plates during operation) to minimize the neutron-induced swelling. As Table I indicates, in absence of pipes, the design satisfies the radiation limits [1] for the 2.7 MW/m^2 peak NWL in the divertor region. The aim of this study is to examine the effectiveness of the shielding scheme proposed for the He-access pipes, estimate the radiation damage at the shield, manifolds, VV, and magnet, and assess the radiation environment behind the magnet due to neutron streaming through the He-access pipe.

We began the multi-dimensional analysis by modeling a simple straight pipe with 30 cm inner diameter (ID) using the DANTSYS code [2] in 2-D R-Z geometry. Based on the preliminary 2-D results, the pipe configuration was modified with shielding plug and inserts, hoping to eliminate the streaming problems. A 3-D analysis was judged necessary to handle the more complex, new pipe configuration. The main transport code used for the 3-D analysis is the Attila 3-D deterministic code [3]. The results of Attila for the damage along the pipe wall were compared to the 3-D DAG-MCNPX Monte Carlo code, currently under development at the University of Wisconsin-Madison [4]. This comparison was performed to demonstrate the applicability of

Table I. Nominal radiation damage and flux in absence of He-access pipes.

	Nominal Values	Design Limits	Allowable Peaking Factor
dpa at shield (dpa @ 40 FPY)	135	200	1.5
He production at manifolds (He appm @ 40 FPY)	1	1	1
He production at VV (He appm @ 40 FPY)	0.2	1	5
Fast neutron fluence @ magnet (n/cm^2 @ 40 FPY)	0.2×10^{19}	1×10^{19}	5
Neutron flux outside magnet (n/cm^2.s)	$\sim10^{7}$	$\sim5\times10^{7}$	5

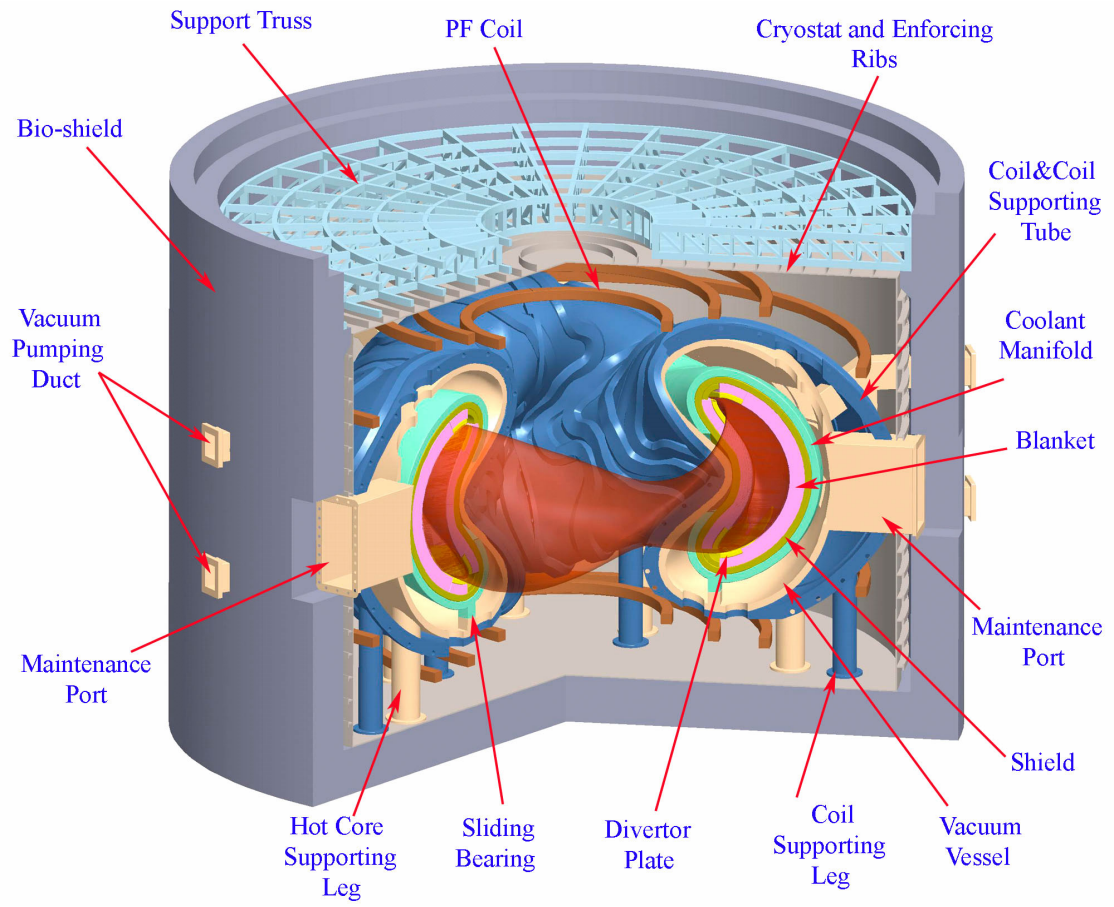

Figure 1. Isometric view of ARIES-CS power plant (average major radius = 7.75 m).

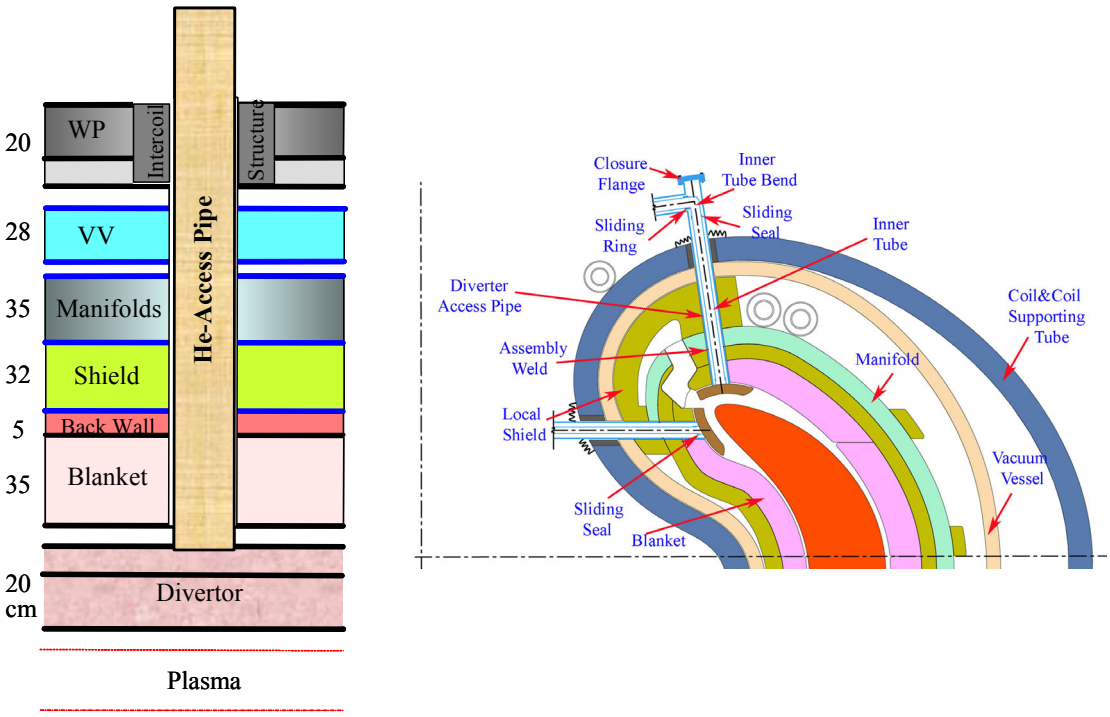

Figure 2. Two-dimensional model for He-access pipe penetrating blanket, shield, manifolds, VV, and inter-coil structure of magnet.

Attila to perform 3-D nuclear analyses of complex fusion systems and in particular the difficult problem of radiation streaming.

2-D Model and Preliminary Results

The 2-D R-Z model is shown in Fig. 2 for the straight He-access pipe and its accommodation in the ARIES-CS design. The pipe begins behind the divertor and extends outward through the blanket, shield, manifolds, VV, and inter-coil structure of the magnet. The divertor system is 20 cm thick and extends 7 m toroidally and 2 m poloidally. The inner layer of the magnet is 1.62 m from the inner divertor surface. Around the pipe, the replaceable blanket can be extended radially to provide extra protection for the permanent bulk shield, if needed. Table II presents the material compositions for the ARIES-CS power plant components.

Figure 3 displays the 2-D results and indicates the peaking in damage to the surrounding components relative to the nominal value, away from the pipe. The analysis identified the following streaming-related problems:

- Shield surrounding pipe is not life-of-plant component
- Manifolds and VV close to pipe are not reweldable
- Winding pack should be located ~40 cm from pipe
- Flux at end of pipe is excessive ⇒ protect externals with local shields.

Table II. Material compositions for ARIES-CS components.

Nominal First Wall (3.8 cm)	Nominal Blanket (54.3 cm)	Back Wall behind Blanket (5 cm)	Pipe Shielding Inserts (10-20 cm)
36% Ferritic Steel	79% Lithium Lead Coolant	80% Ferritic Steel	100% Tungsten Carbide
66% Helium gas	7% Silicon Carbide	20% Helium gas	
	6% Ferritic Steel		
	8% Helium gas		
Blanket behind Divertor (35 cm)	Divertor Zone-1 (3.8 cm)	Divertor Zone-2 (16.2 cm)	Bulk Shield (32 cm)
75% Lithium Lead	21% Tungsten	36% Ferritic Steel	15% Ferritic Steel
9% Silicon Carbide	18% Ferritic Steel	64% Helium gas	75% Borated Ferritic Steel
8% FS	61% Helium gas		10% Helium gas
8% Helium gas			
Manifolds (35 cm)	Vacuum Vessel (28 cm)	Magnet (20 cm)	
52% Ferritic Steel	28% Ferritic Steel	95% JK2LB Steel	
22.7% Lithium Lead	49% Water	5% Liquid Helium	
24% Helium gas	23% Borated Steel filler		
1.3% Silicon Carbide			

To solve the identified streaming problems, four design options were proposed for the He-access pipe [5]. These designs are displayed in Fig. 4 (A – D). The modified pipe starts at the divertor with 30 cm ID and ends with 60 cm ID. The pipe wall is 5 cm thick. A tungsten carbide (WC) hield was added inside the pipe in the form of a plug and shielding inserts around the inner surface of the pipe to protect the surrounding components. A 2 cm wide assembly gap surrounds the pipe. Figure 4 (D) was judged the most promising design for attenuating the streaming neutrons and selected for further analysis using the 3-D Attila and DAG-MCNPX codes as discussed below.

3-D Geometry, Modeling, and Neutron Source

In ARIES-CS, the FW and surrounding in-vessel components conform to the plasma, as shown in Fig. 1, and deviate from the uniform toroidal shape of a tokamak in order to achieve compactness. Within each field period, which covers 120 degrees toroidally, the configuration changes from a bean-shape at 0° to a D-shape at 60°, then back to a bean-shape at 120°, continually switching the surfaces from convex to concave over a toroidal length of ~17 m. To simplify the geometry for the 3-D neutron streaming analysis, the stellarator geometrical configuration was approximated by a torus with 7.75 m major radius and 1.7 m minor radius. Only the upper half of a 45° degree sector of the torus was modeled to decrease the memory and computational time. The 3-D model comprises one fourth of the divertor system with one of its four He cooling pipes. To enhance the accuracy of the solution, the mesh in Attila was translated and rotated so that the centerline of the pipe was aligned with the x-axis. The rotation was performed because the Triangular Chebychev Legendre quadrature set has more nodes near shallow angles. Because of the rotation and constraints with the Attila code, albedo (white)

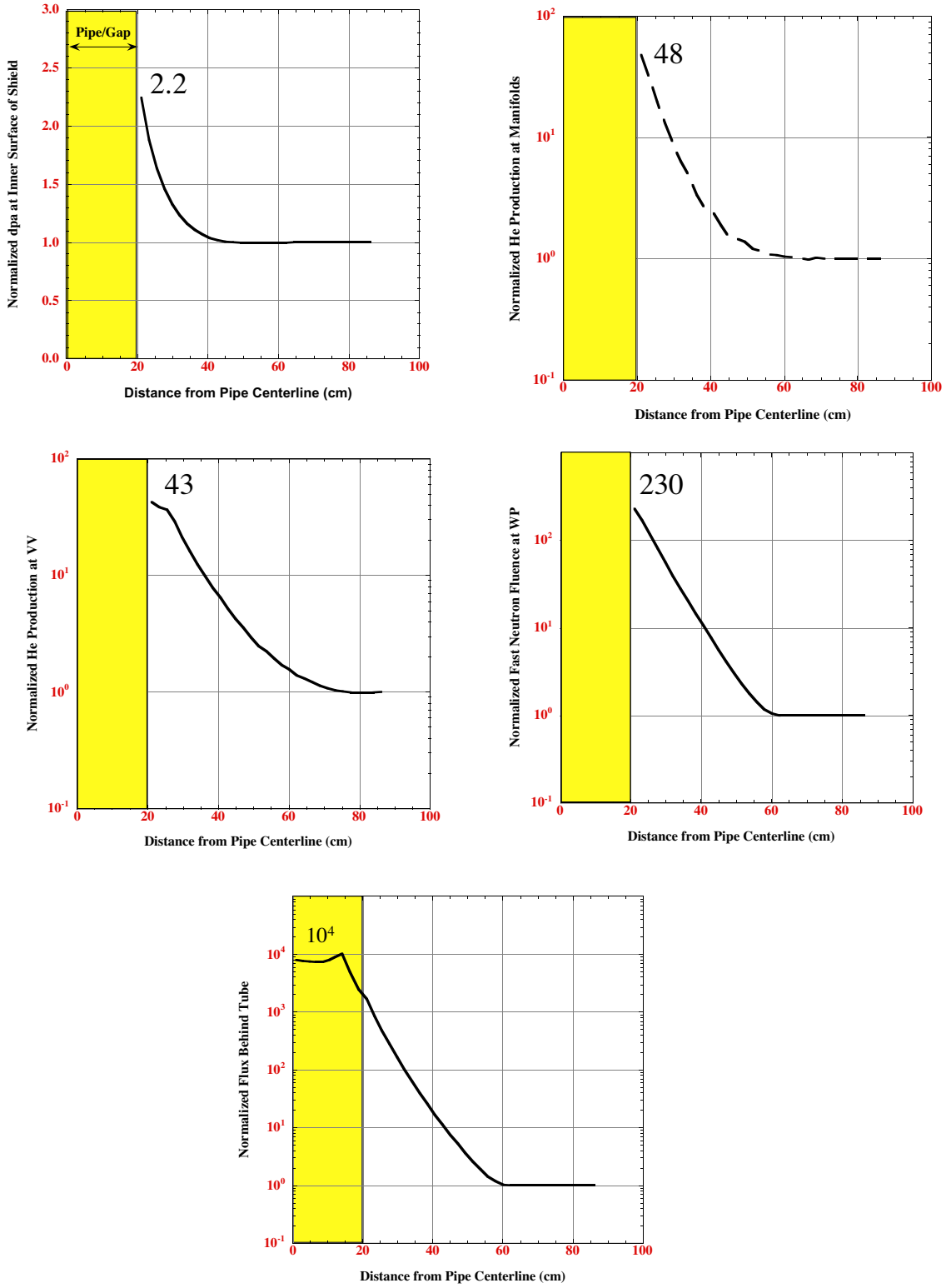

Figure 3. Normalized 2-D results for dpa at shield, He production at manifolds and VV, fast neutron fluence at magnet, and neutron flux at end of pipe.

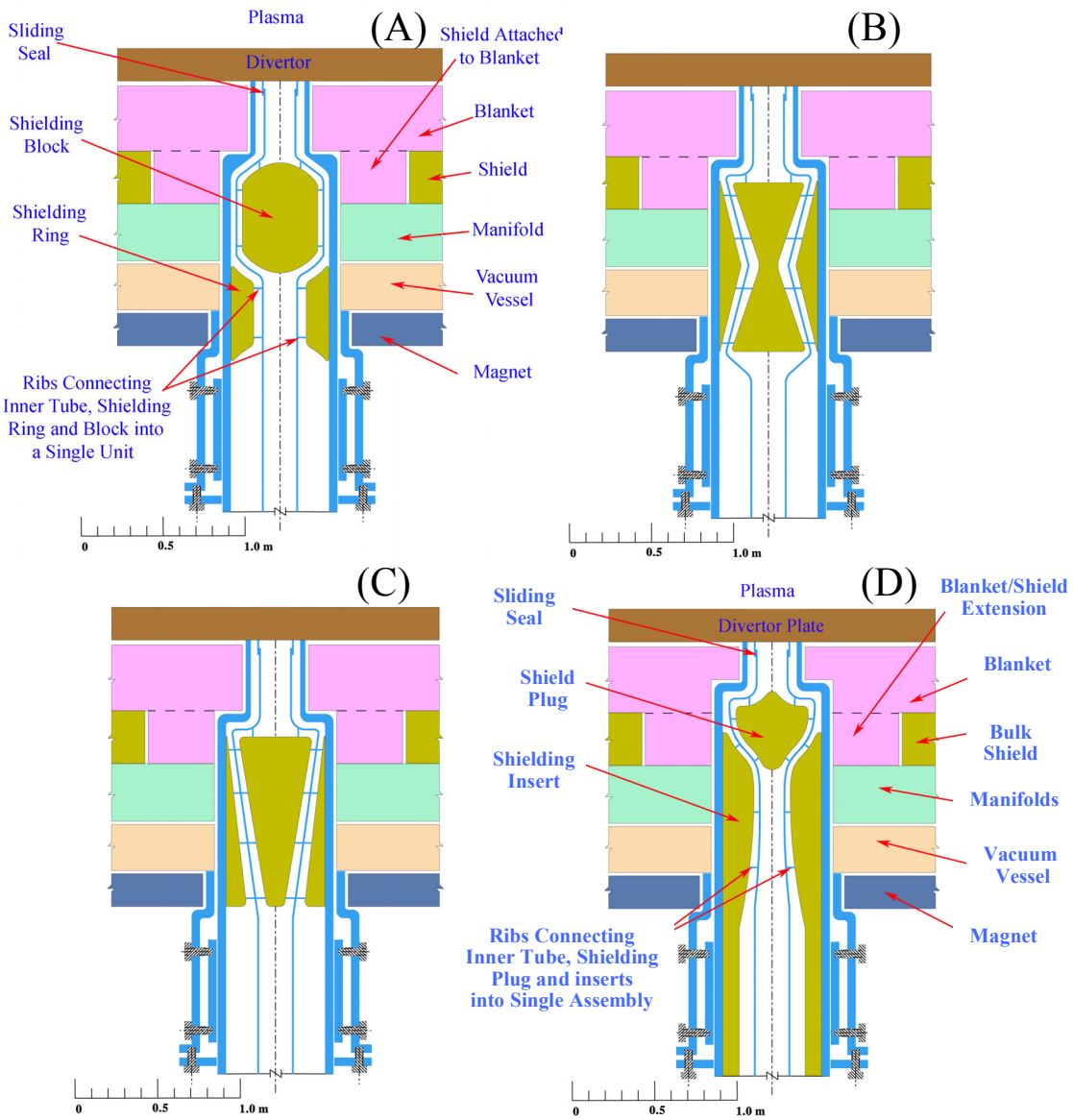

Figure 4. Radial cross sections through four proposed designs of He-access pipe.

boundaries were used for all flat surfaces to simulate the whole torus instead of the reflective boundary condition. A second model without the pipe was generated for comparison to assess the peaking in damage due to neutron streaming through the pipe. The axis rotation was performed for both cases (with and without pipe) to present a fair comparison between results. The CAD models were developed in CUBIT – a U.S. Department of Energy funded software program developed at Sandia National Laboratories [6]. Figure 5 shows the cross section for the CAD model developed for the 3-D nuclear analysis of the pipe case.

To be consistent with meshing for discrete ordinates codes and to improve the numerical and flux convergence, all components were layered in the radial direction for the Attila code calculations. This was done to better resolve the strong flux gradients in the radial direction.

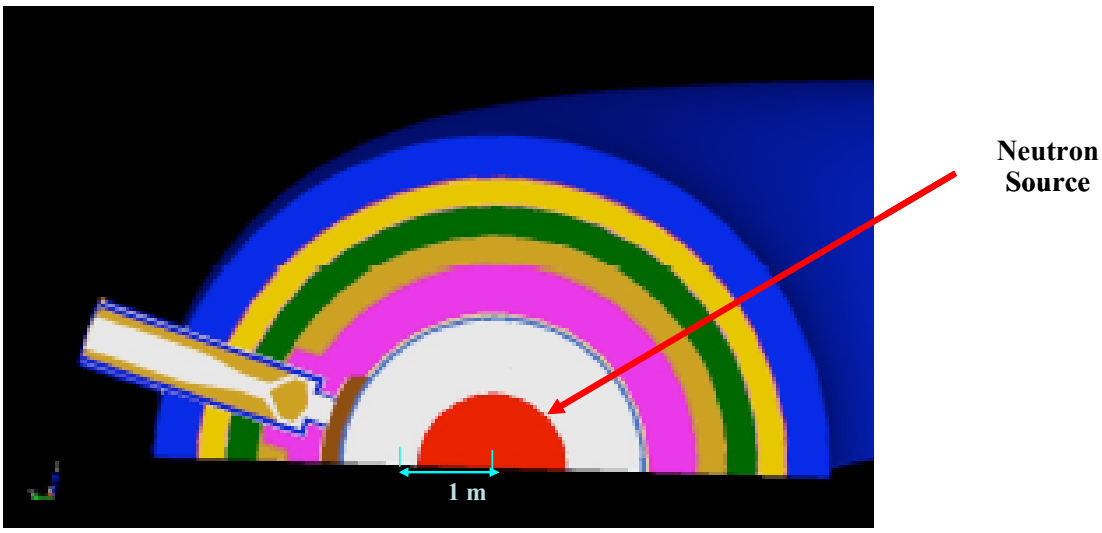

Figure 5. CAD model developed for nuclear assessment of pipe case.

Using this layering, highly anisotropic elements that have small dimensions in the radial direction and coarse sizes in the toroidal direction were created during the mesh generation. Figures 6 and 7 show the CAD models for both cases (with and without pipe) after layering.

The neutron source within the plasma region was approximated by a step function that covers nearly half of the plasma in the radial direction and spans the entire toroidal direction. This simple source configuration was chosen because the ARIES-CS neutron source distribution peaks near the plasma axis. In addition, the actual source does not have any toroidal or poloidal symmetry and the complex mathematical neutron source representation does not lend itself to any of the standard curvilinear coordinates. The step function approximation was set for all of the cases to provide a fair comparison.

To measure the effect of neutron streaming through the pipe on the dpa at the shield, a special model was developed without replacing the shield with the blanket extension. This model was truncated after the manifold to speed up the calculations.

Cross Section Library

The IAEA FENDL 2.1 cross-section library [7] was used for the 2-D and 3-D analyses. FENDL-2.1 is a comprehensive nuclear data library for fusion applications, consisting of 71 materials relevant for fusion components. It is developed in the frame of the international effort coordinated by the IAEA Nuclear Data Section and released for use by the fusion community in December of 2004. The library is a coupled neutron and gamma library in pointwise energy for Monte Carlo calculations and 175 neutron and 42 gamma energy groups in AMPX format for discrete ordinate calculations. The neutron and gamma energy group library is produced by ENEA-Bologna for nuclear fusion applications [8]. Due to the intensive computational time and

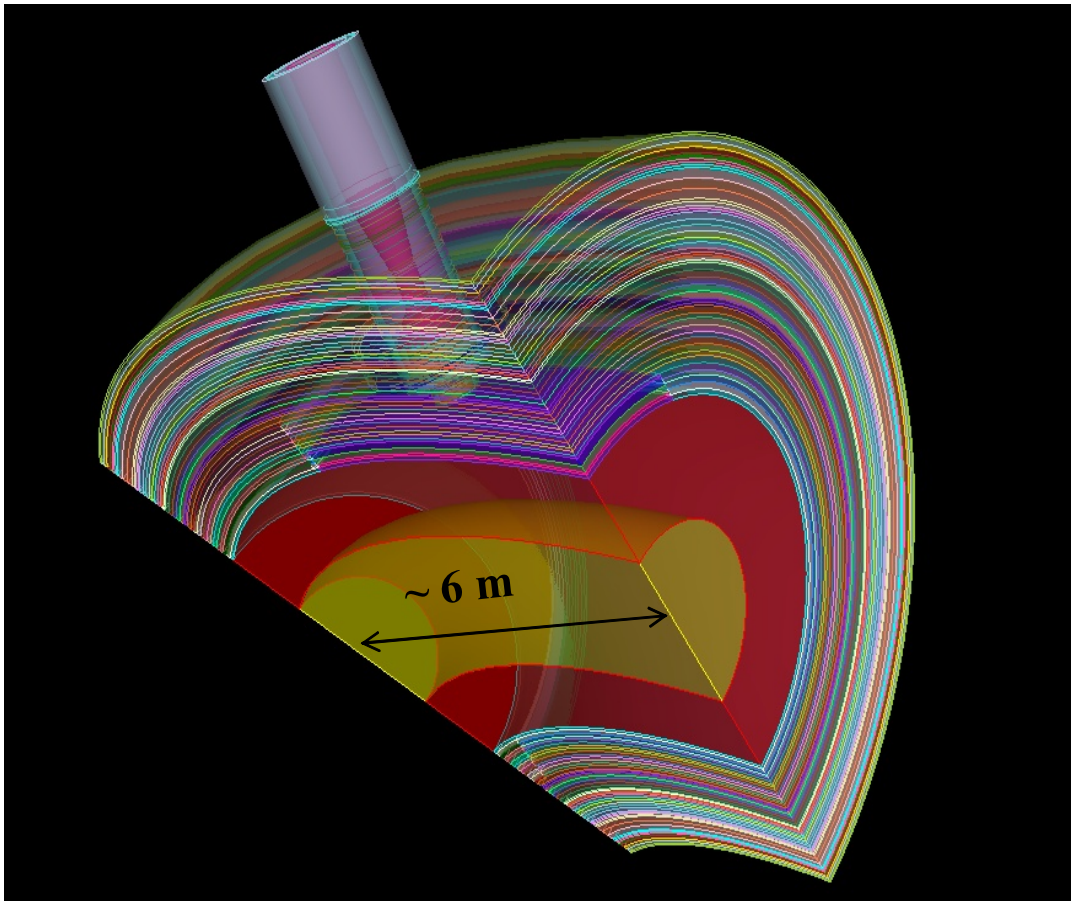

Figure 6. The pipe case after layering.

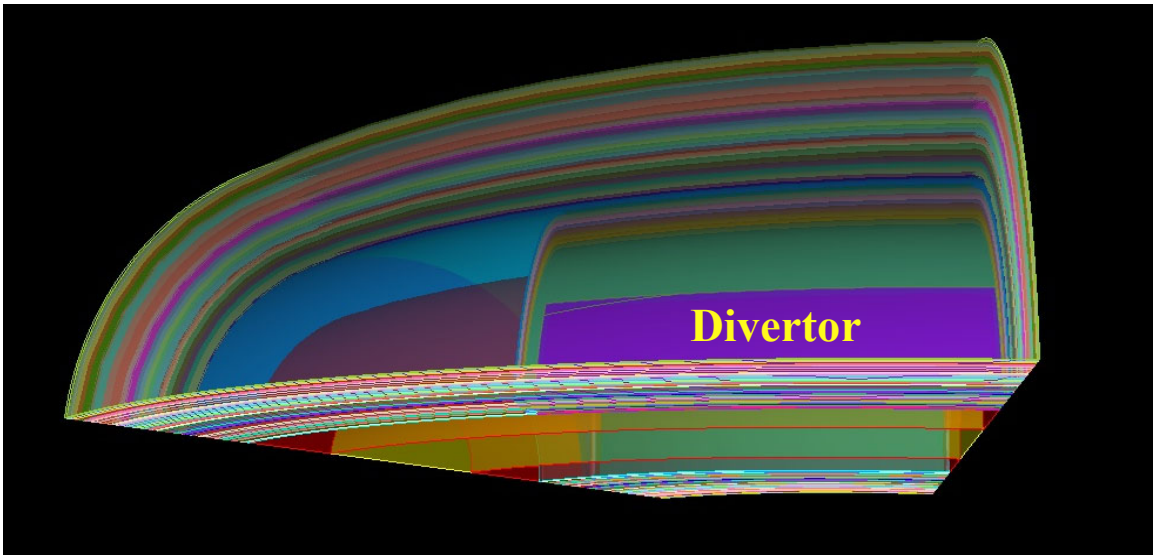

Figure 7. The case without pipe after layering.

memory demands of Attila, the code collapsing capability was used to collapse the 175 neutron energy groups to 46 energy groups and only the impacts of neutrons were considered in this analysis (no gamma ray analysis was performed). Two to five cm thick steel layers were modeled separately to estimate the peak damage at the innermost surfaces of all components and the compositions of Table II were adjusted accordingly.

Methodology and 3-D Codes

The main radiation transport computational tool used for the 3-D analysis is the Attila deterministic transport code [3]. Attila is a numerical modeling and simulation code designed to solve the linearized Boltzmann transport equation for a wide variety of radiation transport applications. It is a 3-D, multi-group, S_n particle transport code with arbitrary order anisotropic scattering. The transport equation is solved in first order form using a tri-linear discontinuous spatial differencing on an arbitrary tetrahedral (tet) mesh. The overall solution technique is source iteration with diffusion synthetic acceleration (DSA) of the scattering source. Attila's solution methodology is based on the traditional Spherical Harmonics expansion of the angular flux, angular integration using accurate numerical quadrature sets, a multi-group energy representation, and Legendre polynomial expansion of the differential angular scattering cross section. Attila imports a CAD model that can be generated from one of several major CAD software packages and generates a tetrahedral mesh based on length parameters provided by the user. Figure 8 shows the mesh generated by Attila for the pipe case.

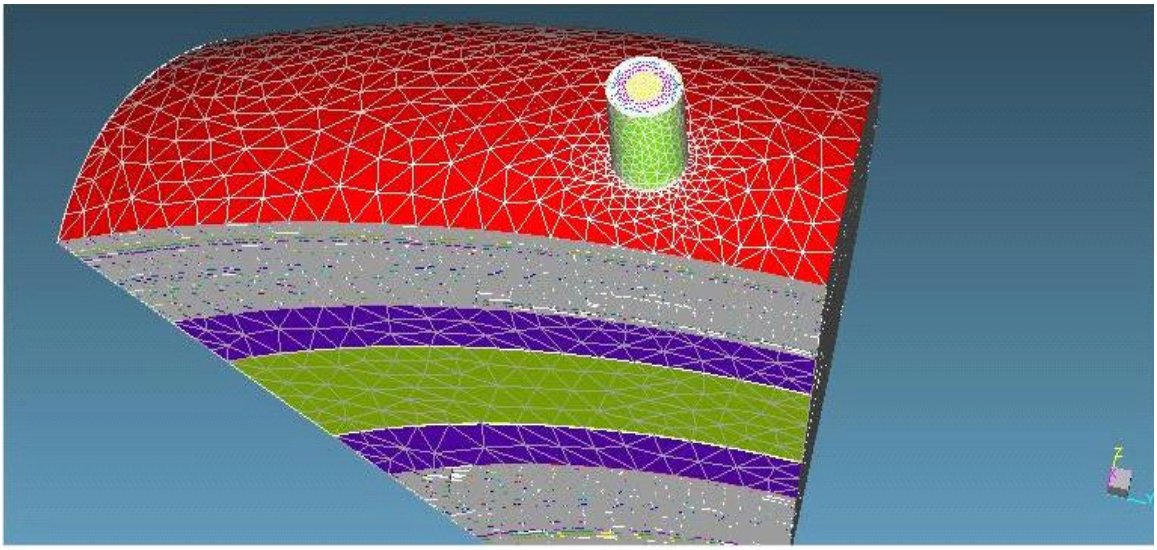

Figure 8. The tetrahedral mesh created in Attila.

Two-dimensional surfaces within this mesh can be formed as assemblies of triangular faces of the tets. Attila uses a linear discontinuous finite element (LDFE) spatial differencing. LDFE has the diffusion limits; there is no need to keep the mesh cell size small relative to a particle mean free path in order to produce accurate results. All that is required is to refine the mesh where the solution is rapidly changing (in the direction of large gradients in the solution). Abrupt changes

in material properties and the resulting solution boundary layers are efficiently handled by the discontinuous aspect of the spatial differencing. More accurate solutions and better solver behavior are generally obtained on meshes, which contain cells with moderate aspect ratios. However, cells with aspect ratios of a thousand to one or more can be used if needed [3]. The layering of several components of the ARIES-CS power plant in the CUBIT CAD model provided mesh cells with high aspect ratios that reached 80-100 for some mesh cells.

The number of mesh cells for the ARIES-CS model was about 276,000. The global mesh size used for most of the regions was 0.4 m. Smaller mesh sizes were specifically assigned to important regions within the pipe, in the vicinity of the pipe, and near high flux gradients. The pipe, shielding plug, shielding inserts, and air volume had mesh sizes that were 7.5 cm or smaller. The regions surrounding the pipe had mesh sizes between 12.5 cm to 30 cm. For 46 neutron energy groups, a S_n order of 24 and a P_ℓ order of 3, using a 12 GB RAM 64-bit machine, the calculational time for Attila to obtain a solution for this model was 23 days.

Attila writes the angular flux moments file at the end of each calculation for post-processing (called reports) of the scalar flux and flux related quantities (information). Post-processing times were negligible with respect to the calculational time except when using the last collided option. The last collided calculation took several days to run, depending on the number of mesh points and angles that have to be evaluated.

Some results obtained by Attila were compared to the University of Wisconsin-Madison's newly developed CAD-based Monte Carlo code (DAG-MCNPX) [4], which is based on the widely used MCNPX code [9]. The DAG-MCNPX code uses a direct CAD-based geometry approach for Monte Carlo analysis. A geometric model is developed and represented in CAD and this model is directly used in particle transport instead of the traditional second order surface geometry representation used in the standard MCNPX code. The ACIS engine (the 3-D modeling kernel (or engine) used by CAD) is linked directly to the Monte Carlo code and used to evaluate particle paths through the geometric domain. For the DAG-MCNPX code, the Common Geometry Module [10] is used to access geometry in the ACIS modeling engine. This model is processed further to generate a facet-based Oriented Bounding Box Tree, which speeds up the ray tracing computations. The ray tracing and other functionality for direct CAD-based Monte Carlo analysis is packaged in a library named DAGMC for Direct Advanced Geometry Monte Carlo. The library depends on the CGM and MOAB [11] open-source libraries, as well as on the ACIS commercial solid modeling engine. DAGMC is linked to the MCNPX Monte Carlo transport code [9] to form the DAG-MCNPX code [4].

DAG-MCNPX requires some preparation in CUBIT [5] before importing the model (ACIS format) into the code. These preparations involve the creation of a volume surrounding the geometry called the complement. The complement consists of all of the "black space" (void regions) within the geometry. Another volume called the graveyard surrounding the complement should also be created. This volume represents the outside world and particles that make their way to this region (cell) will have an importance of zero and are terminated. In DAG-MCNPX, the materials and densities for all non-void cells could be specified in CUBIT. The MCNPX input file does not have to include any cell or surface cards.

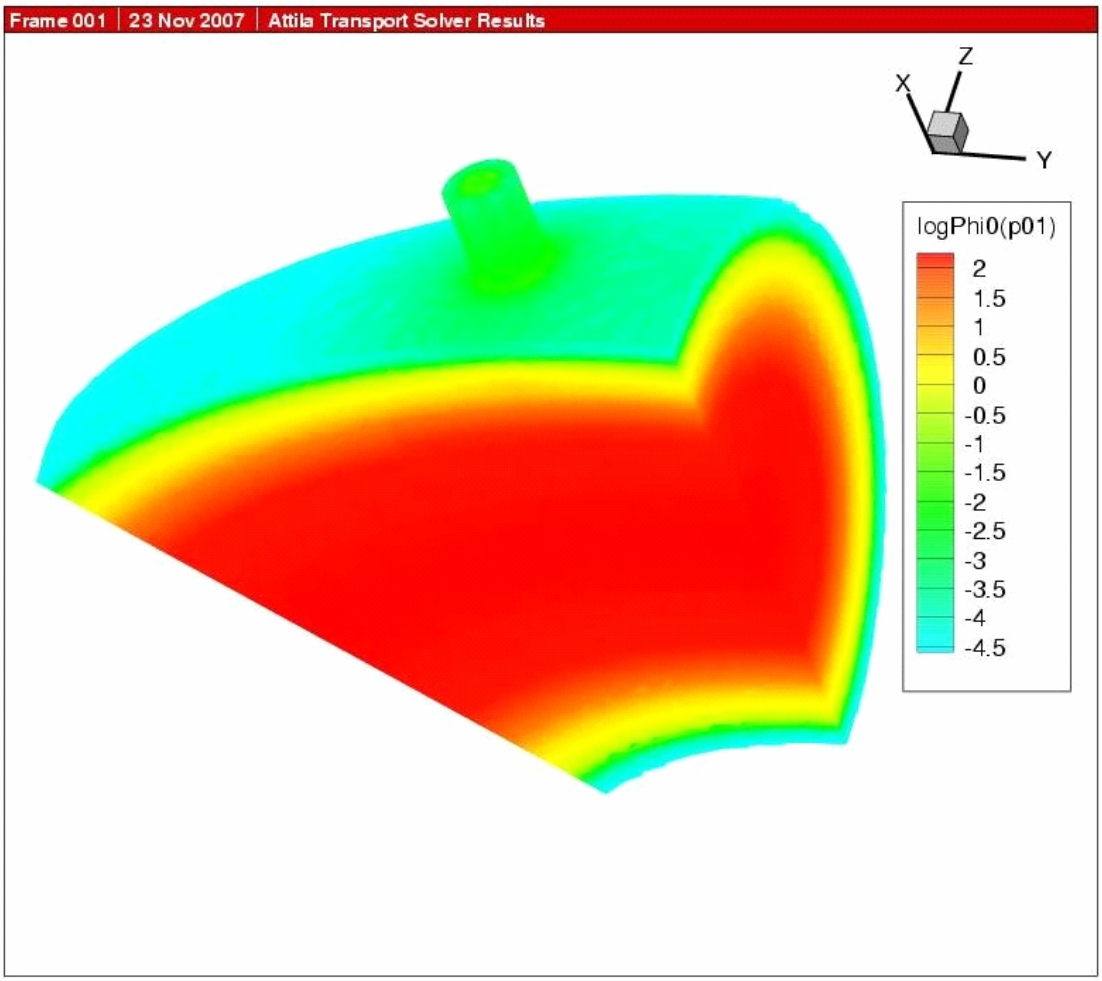

Figure 9. The total flux map throughout the system (relative values; log scale).

3-D Results

Figure 9 depicts a relative total neutron flux distribution map for the whole system. The nominal flux changes by ~6-7 orders of magnitude throughout the system from the divertor to the back of the magnet. The radiation streaming causes ~4 orders of magnitude increase in the total flux inside the pipe, behind the magnet compared to the total flux value (~10^7 n/cm^{2}s) at the well shielded region behind the magnet, far away from the pipe.

Figure 10 shows the relative variation of the total neutron flux along the void inside the pipe and the effect of radiation streaming. The total flux changes by ~4 orders of magnitude along the axis of the 2.7 m pipe. The WC shielding plug causes ~20 fold change in the total flux.

Figure 11, which is based on the special model without blanket extension, shows the dpa across the shield starting from the pipe and moving out in the toroidal direction. Neutron streaming

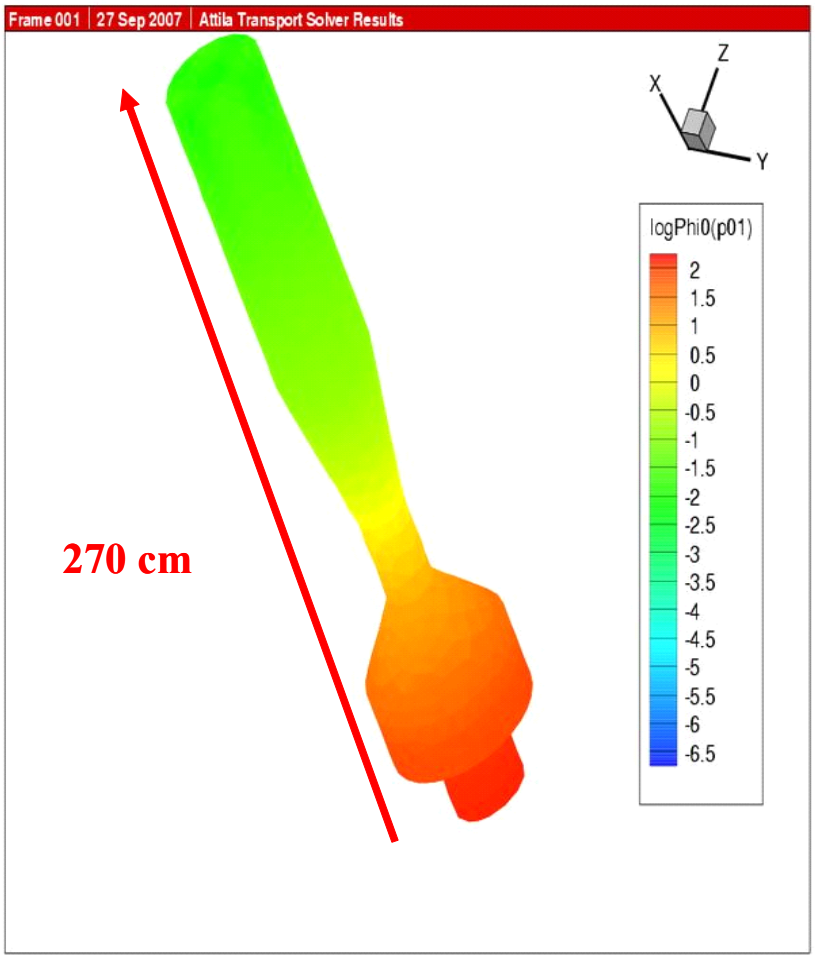

Figure 10. The total flux along the void inside the pipe (relative values; log scale).

through the pipe causes a factor of 1.3 increase in the peak dpa at the shield. The asymptotic value of the peak dpa in the shield was calculated to be 135 dpa @ 40 FPY in the absence of pipes [1] (refer to Table I). With 1.3 peaking factor, the maximum dpa in the shield is therefore 175 dpa over the lifetime of the device. This shows that the bulk shield can be a permanent component and that there is no need for the blanket extension.

Figure 12 shows the He production across the manifolds. The He production increases by a factor of 8.3 due to the neutron streaming through the pipe. The asymptotic value was calculated in the 1-D system and found to be about 1 appm for the expected 40 FPY of operation [1]. According to this analysis, the helium production in the manifolds will reach about 8 He appm in 40 FPY. This is greater than the 1 appm limit of the helium concentration allowed in steel. Rewelding should be avoided in the manifolds in a 40 cm thick region surrounding the pipe.

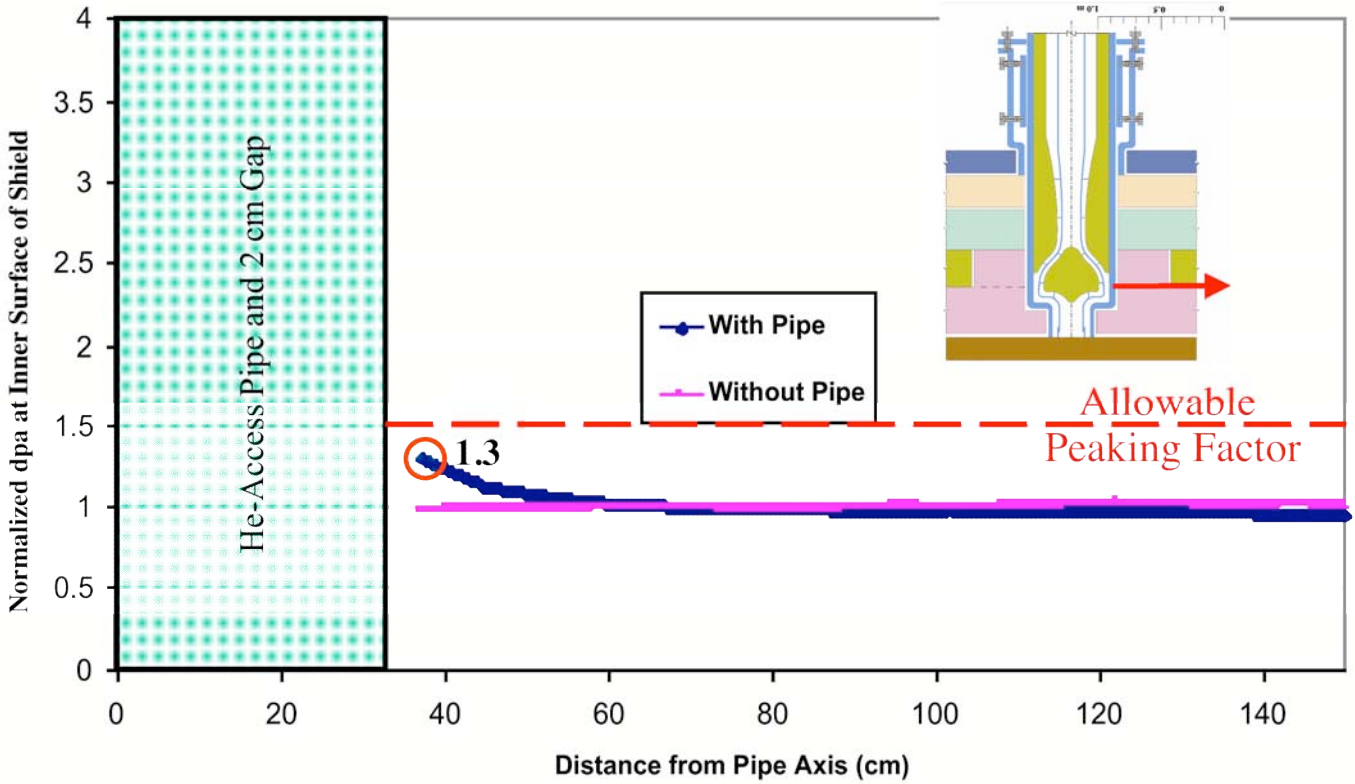

Figure 11. Normalized dpa at shield.

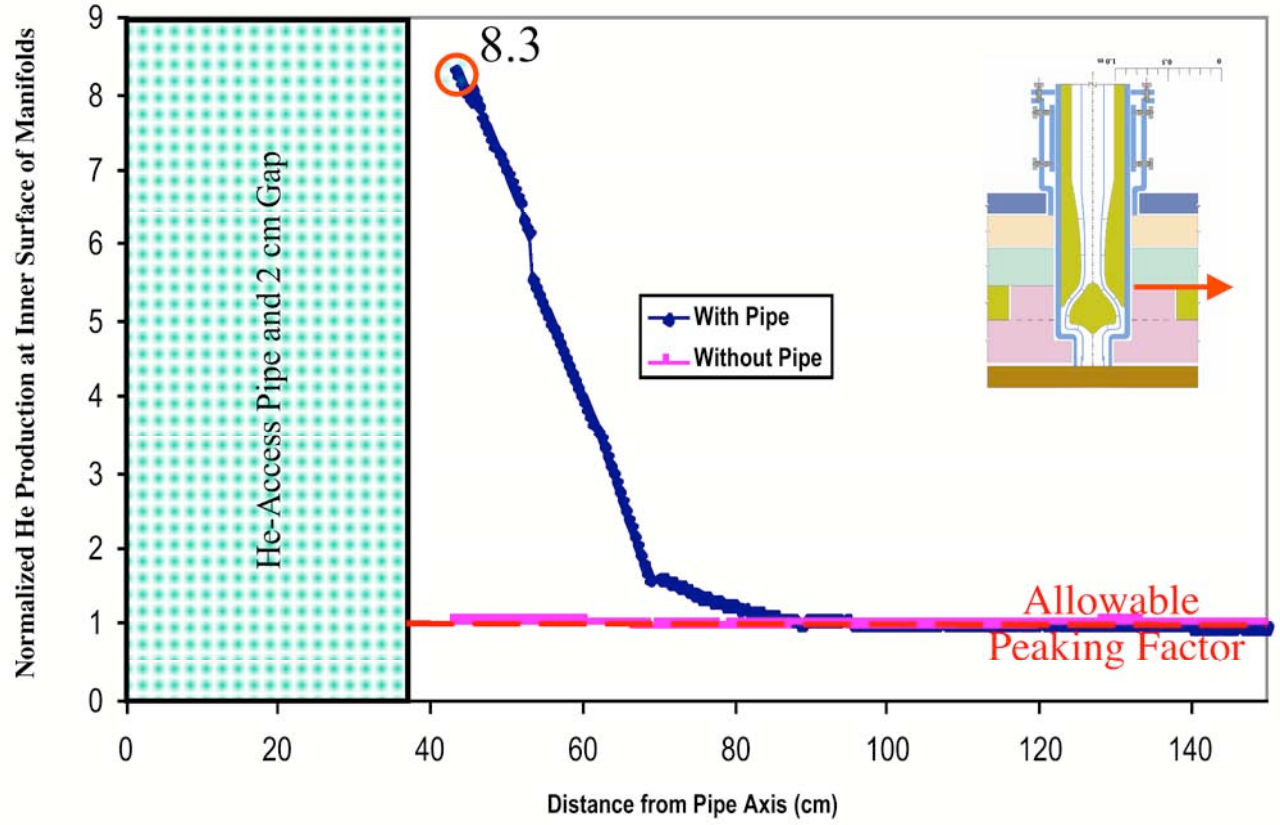

Figure 12. Normalized He production in manifolds.

Figure 13 shows the He production in the vacuum vessel. Comparing the maximum helium production of 1.3 appm to the asymptotic value 0.2 appm indicates that the rewelding should be avoided in a region of a 20 cm thickness surrounding the pipe where the He production is higher than the limit of 1 appm.

Figure 14 shows the fast neutron fluence (E_n > 0.1 MeV) in front of the magnet. The peaking factor of 37 leads to a fluence level of 9 x 10^{19} n/cm^2 after the 40 FPY of operation compared to the asymptotic value 0.2 x 10^{19} n/cm^2. This is 9 times the 10^{19} n/cm^2 limit. The embedded winding pack in the coil structure should be placed 40 cm away from the pipe.

Figure 15 shows the total flux behind the magnet. The peaking factor that exceeds 10^3 calls for local shield (~1 m thick) to surround the pipe end in order to protect the external components against streaming neutrons. The fast neutron flux (E_n > 0.1 MeV) comprises 15-20% of the total flux around the pipe, behind the magnet (refer to Fig. 16).

Figure 17 shows the peaking factors for all response functions. As noted, the peaking factor is more pronounced at the magnet than at the shield. The main reason is that the flux attenuation through the blanket and shielding components falls off much more rapidly than the 1/r variation of the streaming neutron flux within the pipe.

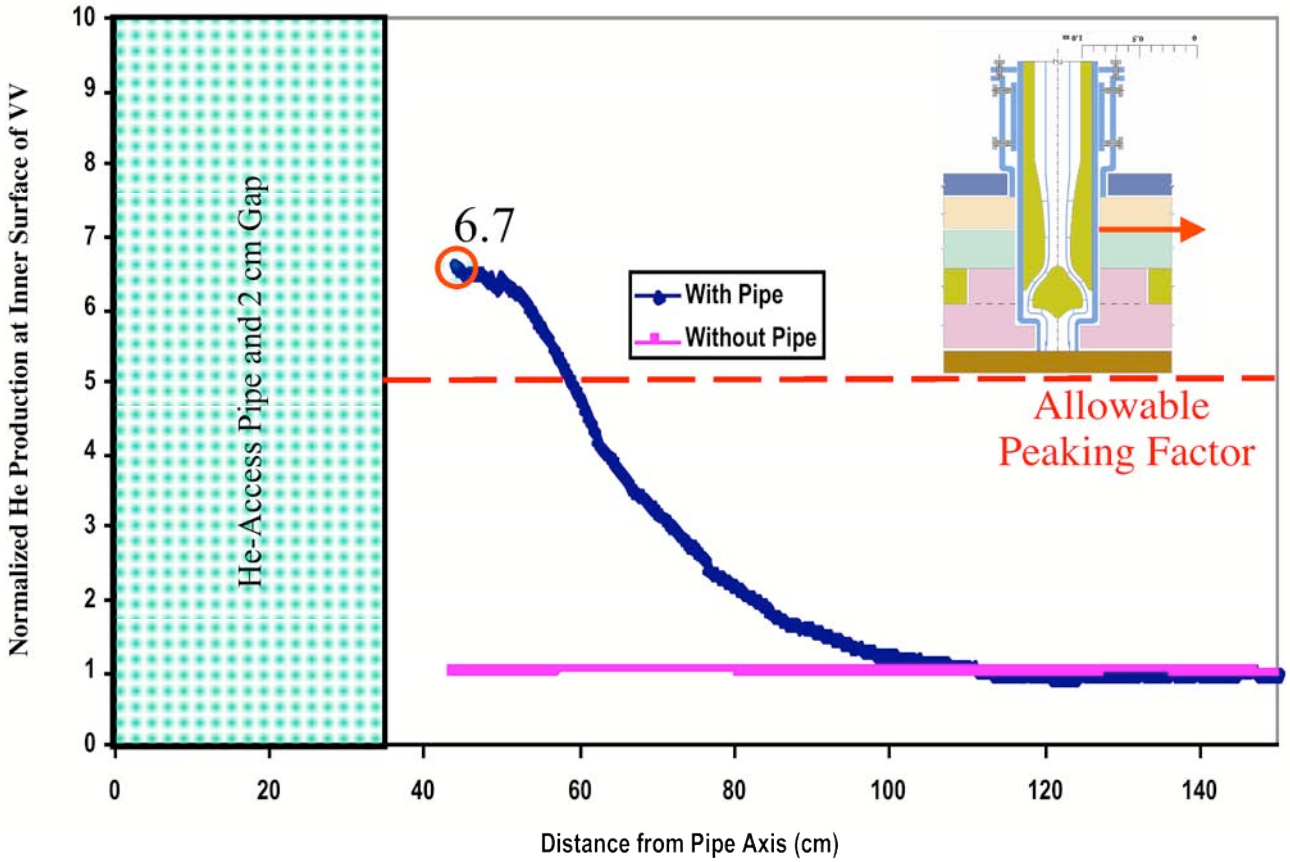

Figure 13. Normalized He production in vacuum vessel.

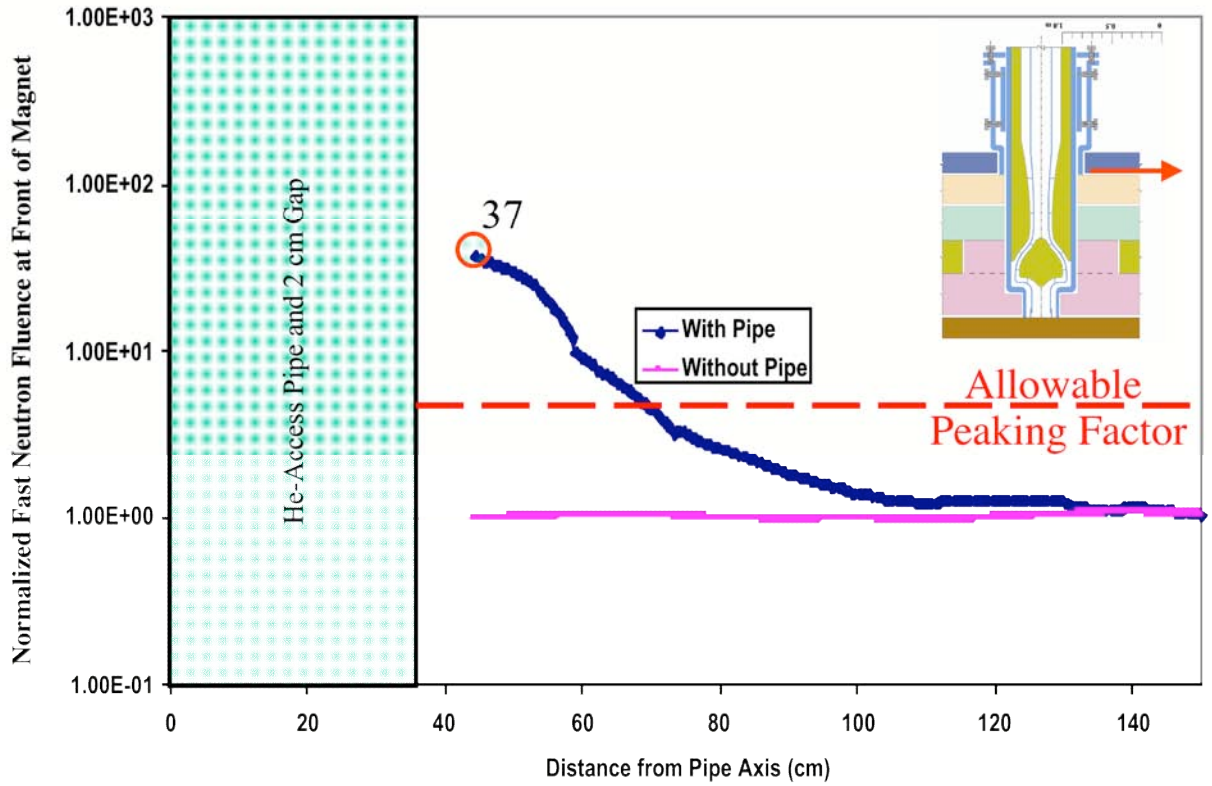

Figure 14. Fast neutron fluence in front of magnet.

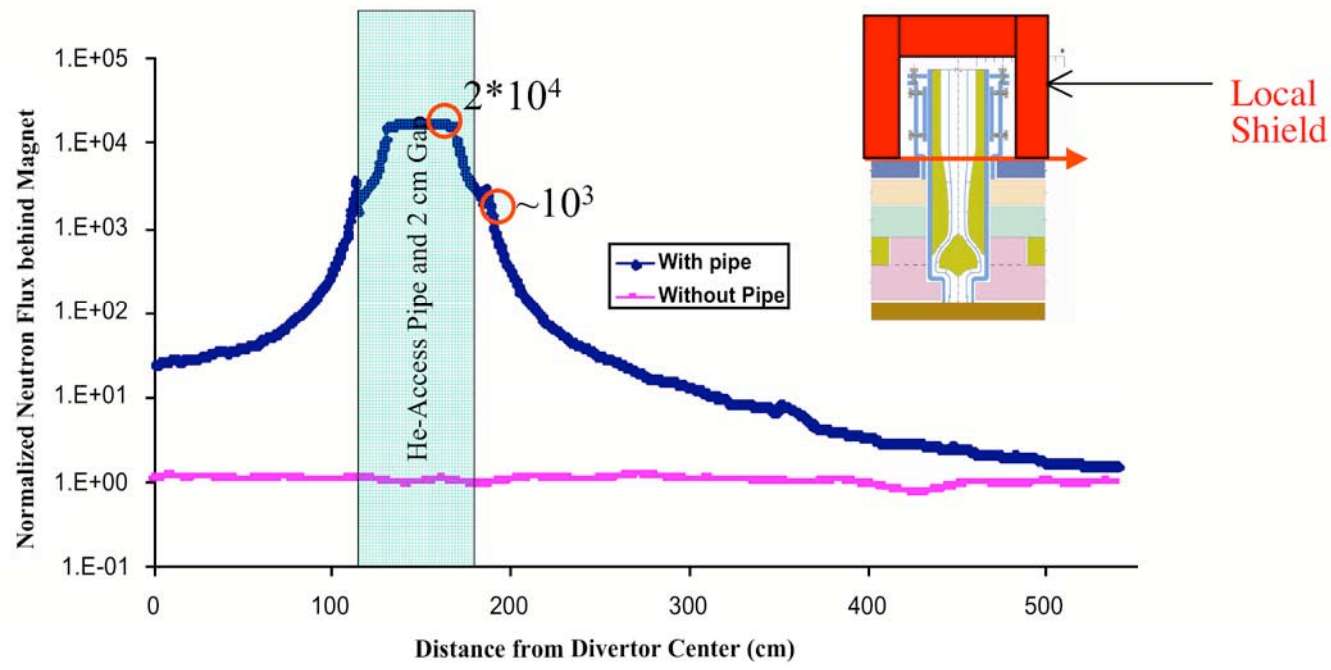

Figure 15. Total neutron flux behind magnet.

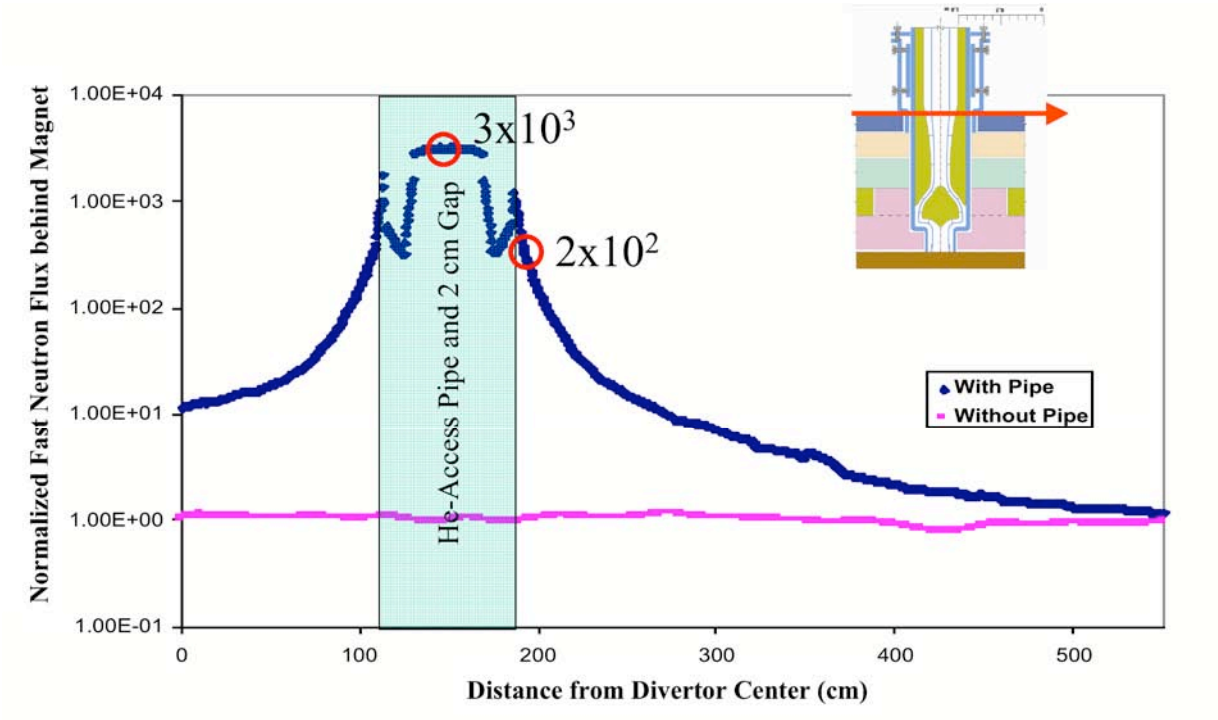

Figure 16. Fast neutron flux behind magnet.

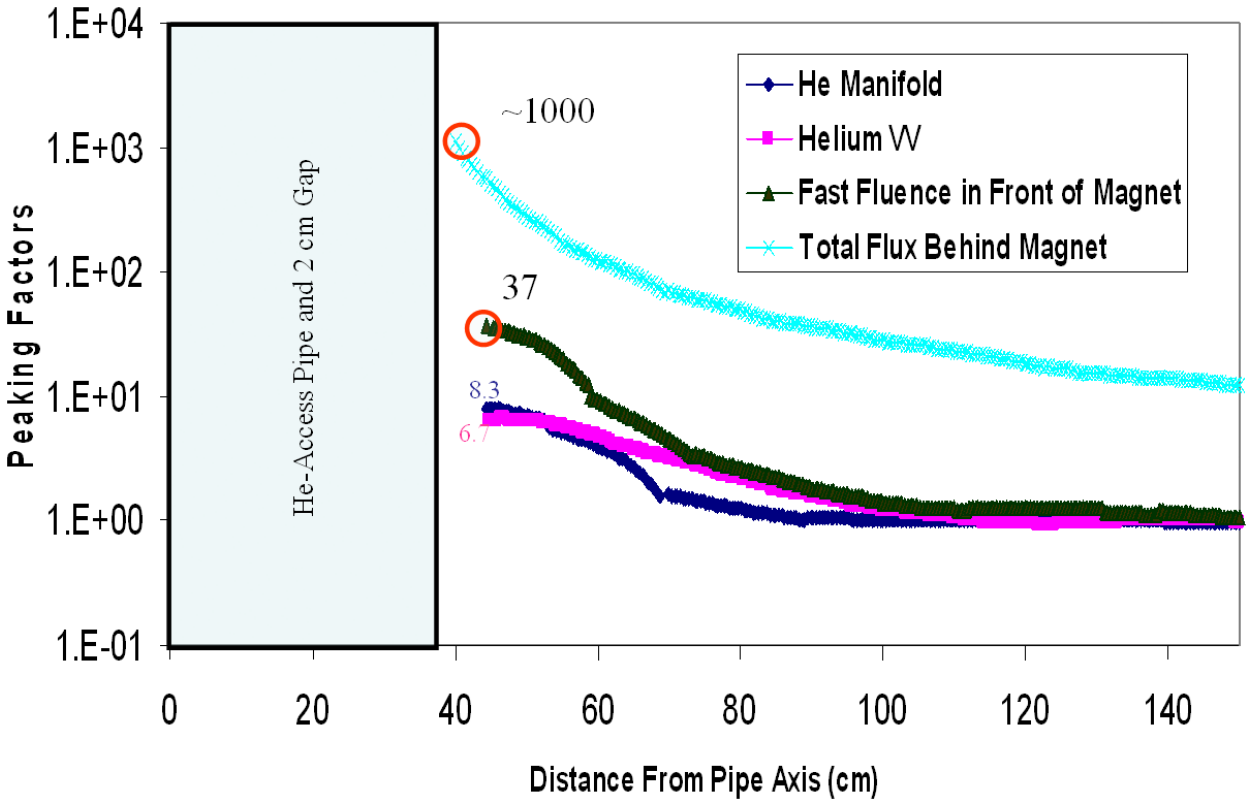

Figure 17. Comparison of peaking factors for all response functions.

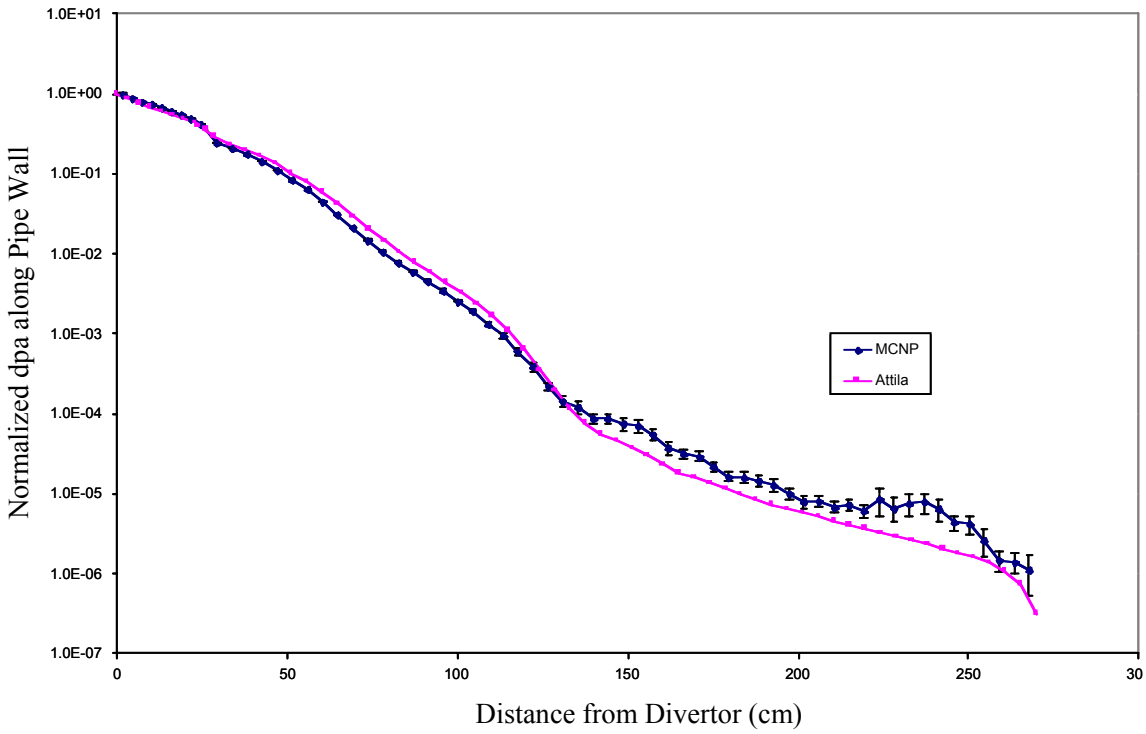

Figure 18. Variation of dpa along pipe wall.

Figure 18 shows the variation of the dpa along the pipe wall. The Attila and the DAG-MCNPX results compare quite favorably over ~1.3 m of the pipe's 2.7 m length. The discrepancy between DAG-MCNPX and Attila near the end of the pipe (seen in Figs. 18 and 19) is difficult to reconcile, as will be discussed later. There is not enough information to judge which solution methodology produces the more correct results.

Examining the results of Figs. 11 and 18, we estimate that the dpa at the pipe wall near the inner surface of the shield could reach ~13 dpa @ 3 FPY – the expected lifetime of the divertor system. At the front of the pipe, the damage is much higher, as Fig. 18 indicates, approaching 130 dpa @ 3 FPY. This means the pipe can operate for 3 FPY without experiencing any structural failure. It can even operate for an extended time (up to 4.5 FPY) before reaching the 200 dpa damage limit.

As noted, the damage near the pipe end (> 2 m) indicates a very low dpa level (< 10 dpa) at the locations of the screws that adjust the divertor plate during operation. Many publications indicated that neutron-induced swelling is negligible below 10 dpa for any type of steel. Normally, a limit of 1% swelling is set for fusion components, corresponding to ~200 dpa for ferritic steel. Assuming a linear fit between 0 and 200 dpa, the 10 dpa level would correspond to 0.05% swelling. Reference 12 confirms this correlation, predicting < 0.05% swelling at 10 dpa. Such a low swelling level should not cause any problem for the screws [5].

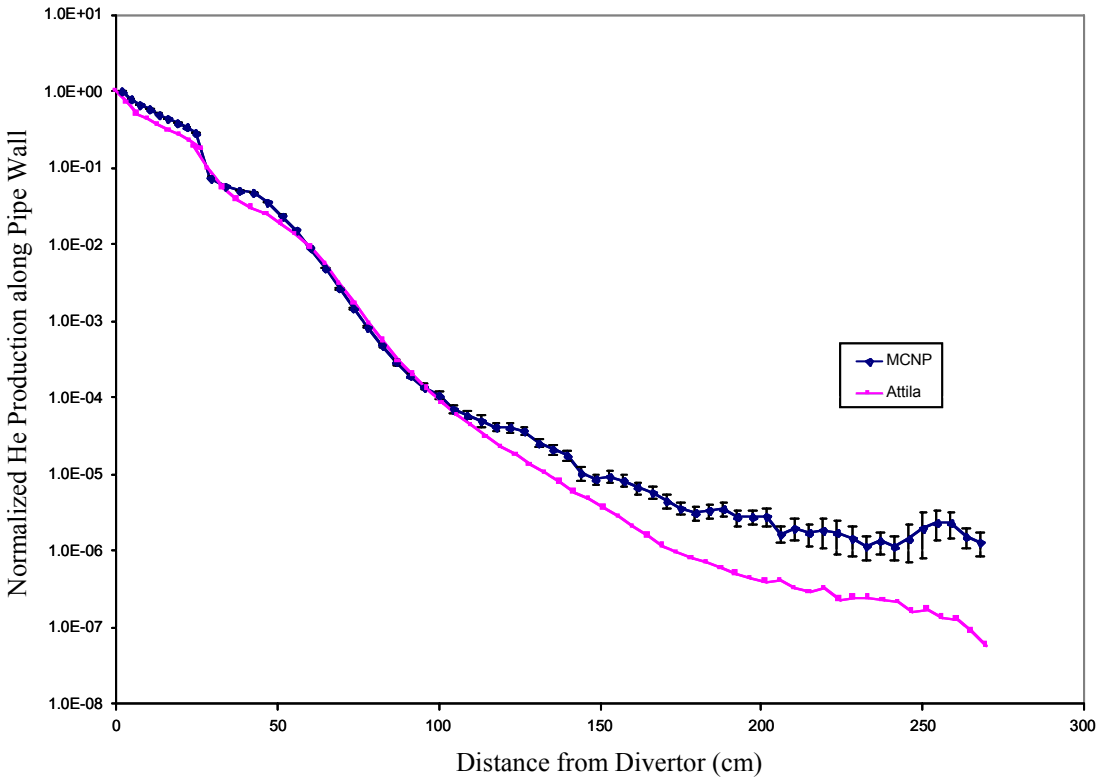

Figure 19. Variation of He production along pipe wall.

Figure 19 shows the variation of the helium production along the pipe wall. Here again the Attila and DAG-MCNPX results compare favorably for the front 1 m of the pipe (near the end of the manifolds). After examining the results of Figs. 12 and 19, we highly recommend replacing the front 60-120 cm of the pipe wall along with the divertor system every 3 FPY for the following reasons:

- He production in the pipe wall reaches approximately 0.6 appm @ 3 FPY near the shield-manifolds interface
- Front ~60 cm of the pipe contains > 1 He appm and cannot be rewelded after 3 FPY and should be replaced with the divertor
- Back of the pipe (> 120 cm) can be reused repeatedly as the He content remains below 1 appm at any time during the 40 FPY of operation
- Middle of the pipe (60-120 cm) reaches the 1 appm limit gradually at various times ranging between 3 and 40 FPY.

Experiences and Challenges with the Attila Code

The Attila 3-D transport deterministic code was the primary computational tool chosen for this work. Our experience with Attila informed us that the code cannot be used as a black box, that is, using Attila without thought going into the CAD modeling of the problem and use of code options and modeling techniques that will facilitate a positive converged flux solution. Problem setup must be approached as one would with any discrete ordinates code and one must be conscious of the method's limitations (ray-effects, use of special techniques for radiation streaming problems, negative flux solutions, etc.). In addition, the computer must have a large amount of RAM to handle large, complex 3-D problems in Attila. With this in mind, the Fusion Technology Institute purchased a new computer with two dual core 3.2 GHz processors and 12 GB of RAM. Additional RAM memory could have been used. To reduce disk swapping and memory requirements for the ARIES-CS pipe streaming analysis and arrive at a solution within a reasonable computational time, we had to collapse the FENDL-2.1 neutron group structure from 175 groups to 46 groups and disregard the gamma transport and analysis. In addition, the x-axis had to be rotated and aligned along the pipe axis centerline to improve the flux results. This rotation negated the use of the reflective boundary option and we had to settle for the albedo boundary option, which meant that we had to discard the results near the albedo boundary. This is a reasonable approximation depending how far the analysis point of interest is from the boundary; but this is not a satisfactory option for a production code. In addition, a number of options were tried to reduce negative fluxes and improve the results such as the first scatter and last scatter options. These options will be discussed in Appendix-A but note that we had little success using these options. The Appendix contains further problems encountered running the code (Appendix-A), and a brief description of the code followed by an extensive list of nuances, difficulties, and attempted remedies for the problem analyzed (Appendix-B).

In summary, a few remarks on the use of the Attila code include:

- Must approach modeling as one would with any discrete ordinates code and be conscious of the method's limitations (3-D problems can be memory intensive, special treatment for radiation streaming problems, ray effects, negative fluxes).
- Computer must have large amount of RAM to handle large complex problems.
- Expertise using Attila must be developed to continually improve the quality of results and avoid using the tool as a "black box".

Experiences and Challenges with the DAG-MCNPX Code

The UW-Madison's CAD-based modeling code, DAG-MCNPX [4], was used to model the complex pipe geometry. However, specific features of this problem led to challenges in accomplishing the necessary calculations. In addition to the generic limitations of Monte Carlo methods for solving deep penetration problems, some additional restrictions are introduced by the use of the DAGMC solid modeling capability. As with most problems of this type, a substantial level of variance reduction and/or a substantial quantity of CPU-time are needed to achieve statistically meaningful results far away from the source. The deep penetration through all components caused the total neutron flux to decrease by ~7 orders of magnitude and the fast flux by ~8. At higher energies the drop of the neutron flux was more severe. The helium

production cross section is effectively zero below 3 MeV. Without any variance reduction, it would have been impossible for MCNPX to produce reliable results, especially for high energy events. This particular problem, a shielded pipe with narrow streaming pathways through thick components, was complicated by the toroidal geometry and the complex profile of the additional shield internal to the pipe. Using the DAGMC capability reduced the ability to segment the geometry successfully, particularly within the pipe, in turn limiting the ability to use geometry-based importance sampling along the pipe. Mesh-based weight windows were available, in theory, but populating such weight windows proved to be challenging in such geometry. The multi-layer CAD model generated for Attila (see Fig. 6) was used to develop a cell-based weight window set for population control for the DAG-MCNPX code. Before generating the weight windows, it was difficult for particles to reach any layer beyond the shield. Hence, the weight window generator produced many zeros, depending on run time. Cell importances were manually changed to maintain constant population between cells and consequently the weight windows were improved. Once the weight windows were generated, the problem ran for ~6 days in order for the statistical error for the He production along the pipe wall to drop below 30% at the magnet level. Such a short run time was achievable by setting the energy cutoff at 3 MeV for the He production. The discrepancy between DAG-MCNPX and Attila near the pipe end (seen in Figs. 18 and 19) is difficult to reconcile. There is not enough information to judge which solution methodology produces the more correct results. There are two potential sources of error:

1- Use of weight window can bias the Monte Carlo results

2- Negative fluxes computed by Attila behind the magnet (see Appendix-A) can reduce the total flux results and lower the damage in the pipe wall.

In summary, similar remarks should be offered for using DAG-MCNPX as were given above for Attila, albeit in a slightly different vein:

- Must be conscious of the method's limitations (deep penetration problems are CPU-intensive and require advanced variance reduction)
- Require substantial computing resources, certainly for CPU time and possibly for RAM although less than Attila
- Expertise using DAG-MCNPX must be developed to continuously improve quality of results and avoid using the tool as a "black box".

Conclusions

We assessed the 3-D streaming problem for a set of four pipes that supply the He-coolant to each divertor system of ARIES-CS. The pipes begin behind the divertor and extend outward through the blanket, shield, manifolds, vacuum vessel, and coil structure. The tools utilized to analyze the 3-D problem are the Attila deterministic code and the DAG-MCNPX Monte Carlo code. Both codes import a CAD model of all components eliminating modeling errors and allowing faster design iterations, if needed.

The proposed pipe design with shielding plug and inserts represents a first-attempt approach that would be maintainable while offering several features that may alleviate the streaming problem. Our 3-D analysis indicated that neutron attenuation through the shielded pipe is not sufficient to eliminate the streaming problems entirely. The main results are:

- Bulk shield is well protected $\Rightarrow$ no need for blanket/shield extension
- Peaking in damage is more pronounced at magnet than at shield
- Helium production at manifolds and VV exceeds reweldability limit by 2-8 fold $\Rightarrow$ avoid rewelding within 20-40 cm from pipe
- Winding pack should be placed at least 40 cm from pipe
- Neutron-induced swelling in screws (that adjust divertor plates during operation) is negligible (< 0.05%)
- Front 60-120 cm of pipe wall is not reweldable and should be replaced along with divertor system every 3 FPY.

The final ARIES-CS design accords with these recommendations [13], calling for no rewelding of the manifolds and VV near the pipe and assuring the coil is located at least 40 cm from the pipe. The neutron flux behind pipe is excessive, mandating additional local shield (~1 m) to protect the externals. This fairly thick local shield is missing in the final ARIES-CS CAD drawings.

Comparing the 2-D results (for simple, straight pipe) with the 3-D results (for the pipe with WC shielding plug and inserts) indicates that the addition of WC shield is ineffective as all streaming problems (at manifolds, VV, magnet, and outside pipe) still exist, except at the shield. Future studies should develop a more effective scheme to attenuate the streaming neutrons and reduce the flux outside pipes. For example, a simple pipe with smaller ID than 60 cm and several right-angle bends represents a better approach, eliminating the need for the massive WC shielding plug and inserts (170 tons for the 24 pipes of ARIES-CS).

References

1. L. El-Guebaly, P. Wilson, D. Henderson et al. "Overview of ARIES-CS In-vessel Components: Integration of Nuclear, Economic, and Safety Constraints in Compact Stellarator Design," University of Wisconsin Fusion Technology Institute Report, UWFDM-1322 (April 2007). Available at: http://fti.neep.wisc.edu/pdf/fdm1322.pdf.

2. R. Alcouffe et al., "DANTSYS: A Diffusion Accelerated Neutral Particle Transport Code System," Los Alamos National Laboratory Report, LA-12969-M (1995).

3. J.M. McGhee, T.A. Wareing, and D.A. Barnett Jr., "Attila Radiation Transport Software User's Manual," Transpire, Inc. (2006). Available at: http://www.transpireinc.com.

4. DAG-MCNPX User Manual. Available at: http://cgi.cae.wisc.edu/~fti/dagmc.cgi/wiki?p=UsersGuide.

5. S. Malang, consultant, Germany, private communications (September 2006).

6. T.D. Blacker et al., "CUBIT Mesh Generation Environment, Vol. 1: User's manual," SAND94-1100, Sandia National Laboratories, Albuquerque, New Mexico, May 1994. Available at: http://endo.sandia.gov/cubit/release/doc-public/Cubit_UG-4.0.pdf.

7. The FENDL-2.1 175 neutron 42-gamma group coupled cross-section library is available at: http://www.iaea.org/.

8. D. López Aldama, "FENDL-2.1, Update of an Evaluated Nuclear Data Library for Fusion Applications." Available at: http://www.iaea.org/.

9. MCNPX Version 2.5.0 User's Manual, LA-CP-05-0369, Los Alamos National Laboratories, Los Alamos, New Mexico.

10. T.J. Tautges, "The Common Geometry Module (CGM): a Generic, Extensible Geometry Interface," Engineering with Computers 17:3 (2001) 299-314.

11. T.J. Tautges, "MOAB-SD: Integrated Structured and Unstructured Mesh Representation," Engineering with Computers 20 (2004) 286-293.

12. Y. Miwa, E. Wakai, K.Shiba, and A.W. Rowcliffe, "Swelling of F82H irradiated at 673 K up to 51 dpa in HFIR," Journal of Nuclear Materials 283-287 (2000) 334-338.

13. L.M. Waganer, R.J. Peipert-Jr, X.R. Wang, and S. Malang, "ARIES-CS Maintenance System Definition and Analysis," to be published in Fusion Science and Technology.

APPENDIX-A

Attila: Negative Fluxes, Options and Considerations for Steaming Problems

Even though the total fluxes in all components are positive, we observed negativities in fluxes of numerous energy groups. For example, Fig. A1-a shows the negativity within and outside the magnet and surrounding the pipe for the first neutron energy group. Similar negativities have been observed for the top 29 energy groups. Other negativities appear inside other components (such as blanket, shield, VV, magnet) but in the lower energy groups (#41-46). Figure A1-b displays the widespread negativities in the blanket and shield for the energy group #44.

A few attempts to fix the negativity problem were not successful. These included decreasing the mesh size, using the last collided flux option, and running the first group with high S_n order and lower S_n order for subsequent groups. The first method increased the runtime and memory significantly. For instance, decreasing the global mesh size by a factor of two increases the runtime by a factor of 6-8. With less than double the mesh cells, we ran out of memory even with the low memory option. This persistent problem of negative fluxes, particularly in the higher energy groups, is of concern and decreases our confidence in the Attila results.

The system investigated here showed that streaming problems may represent an issue that cannot be completely handled in Attila and may require further attention and investigation. More importantly, our results have shown an unrealistic, unphysical rise of the fluxes and reaction rates at the nearest 4-7 cm of the pipe. The unphysical rise was more severe for the helium production (threshold reaction in steel) and the fast neutron flux than for the dpa and the total flux. This may be due to the ray effect, but more investigation is necessary to pinpoint the problem.

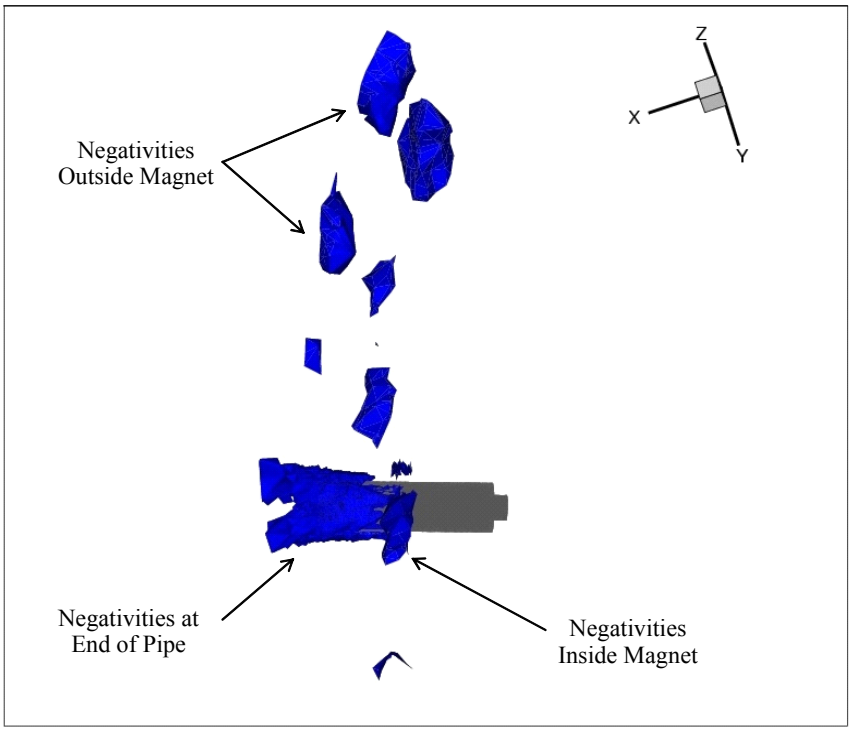

Figure A1-a. Negativity in flux within and outside magnet and surrounding pipe for first neutron energy group (13.5 to 14.2 MeV).

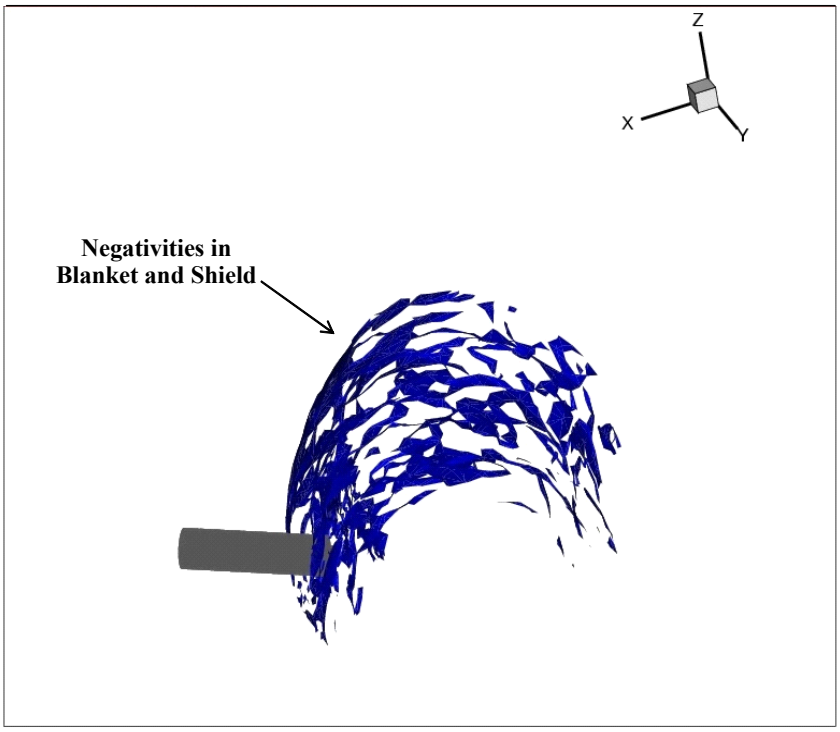

Figure A1-b. Negativity in flux of blanket and shield for neutron energy group #44 (0.88 to 1.86 eV).

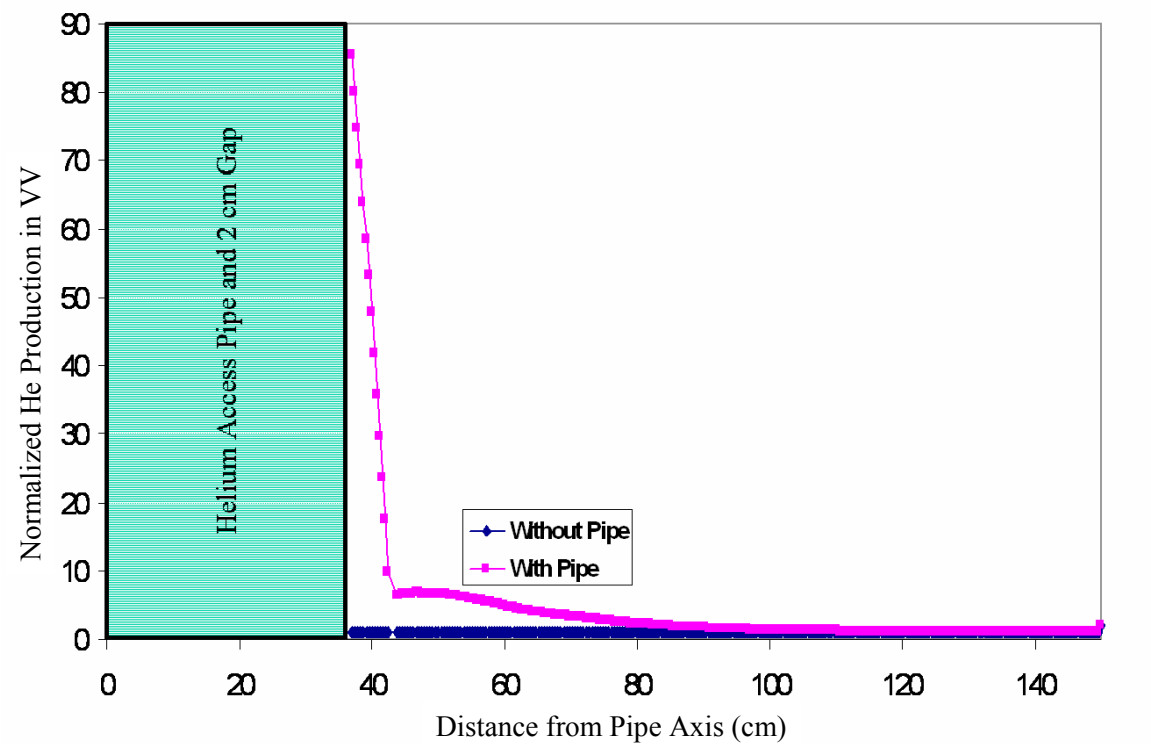

Figure A2. Normalized He production in vacuum vessel.

Figure A2 depicts the unphysical rise of the helium production in the vacuum vessel near the pipe. The results show that the He production in the vacuum vessel changed by a factor of 16 in the first 6 cm of the vacuum vessel starting from the pipe wall. Analytical calculations showed that the helium production reduction should not be more than a factor of 2 over this small distance. A similar behavior was observed for the other response functions, as will be discussed shortly.

Three options were developed in Attila to assist the solution for the streaming problem, but only the last option was relevant to our model. However, it did not provide a satisfactory solution for this problem. The first option is the first scattered distributed source (FSDS) solution technique that can provide significant calculation advantages for certain classes of transport problems. It is based on the concept of decomposing the total solution for a transport problem into two components: 1) the uncollided component, and 2) the collided component. The two components are calculated separately and then the results are summed to produce the total solution. This option proved effective for other problems for Attila experimentations, but its limitation is that it only works with point sources. It uses the ray tracing technique for computing the optical paths and generates a scattered source distribution throughout the system. The second option is the S_n collision source option, which uses a high S_n order calculation for the uncollided neutrons, followed by a lower S_n order for the remainder of the calculations. The S_n option works with volumetric sources, but it does not work with either albedo or reflecting boundaries that are used in our problem. It does not completely solve the problem of streaming since it still uses the S_n method for source particles, but can be satisfactory because of the initial high S_n order (n = 60 for the Triangular Chebychev Legendre quadrature). We tried this source option with vacuum

boundaries but found that our volumetric source could not be modeled correctly without reflecting boundaries. The flux results also contained a large number of negative flux values. The third option is the last collided (LC) edit. Attila integrates the converged scattered source to the point of interest. This technique is effective for calculations where the area of interest is in a low scattering medium adjacent to a scattering medium, where particles stream to the area of interest. The LC edits (reaction and flux) are used in the following manner. First, a standard S_n calculation is performed with a certain quadrature set and order. LC edits can then be performed by traversing the mesh along many individual characteristic lines-of-sight originating from edit locations, using integral transport theory to account analytically for attenuation along the path (due to absorption and scattering). The quadrature set and S_n order used for the LC edit can both be different than the ones used in the standard S_n calculation. The LC method is performed as an edit step, so any number of LC edit calculations can be performed as a report only run after the converged scattering source has been determined [3]. Unfortunately, the Attila code has a rather primitive implementation of the LC method for multiple reaction edits. The code performs a numerical flux integration for each reaction edit rather than computing the flux once and multiplying by the appropriate reaction edit. The use of the LC option for our pipe analysis did not improve the solution. The helium production in the vacuum vessel was higher using the LC option at points close to the pipe than the normal (without LC) calculations. This would be expected, however, the increase was unrealistically large. A further investigation of this should be made.

Figures A3 through A4 show the difference between the results using the LC option and those without the LC option for different points from the pipe surface along the toroidal direction for the different components. The unrealistic rapid decrease of the helium production near the pipe appeared with the LC option as well as without it in both manifolds and VV. In the latter, the LC results were even higher than the normal calculation, which disagrees with the much lower continuous results away from the pipe. The difference between the results with and without using the LC option decreases as we move further away from the pipe until it is totally negligible at about 15 cm from the pipe.

The calculated fast fluence using the LC option decreased by a factor of 30 in the first 7 cm from the pipe (see Fig. A5). This attenuation is unphysical for the steel in this region. The calculated fast fluence using the LC option was about double that calculated without the LC option. The difference between the LC fast fluence and the normal fast fluence decreases as one moves away from the pipe.

Figure A6 depicts the total flux behind the magnet. The decrease in the total flux in the first 4 cm was a factor of 4. The difference between the LC and normal results was about 1.25 at the closest point to the pipe wall but decreased rapidly after a few centimeters. The rapid rise in the first few centimeters was not very severe in the case of the total flux behind the magnet. Scattered neutrons represent the main contribution for the total flux behind the magnet.

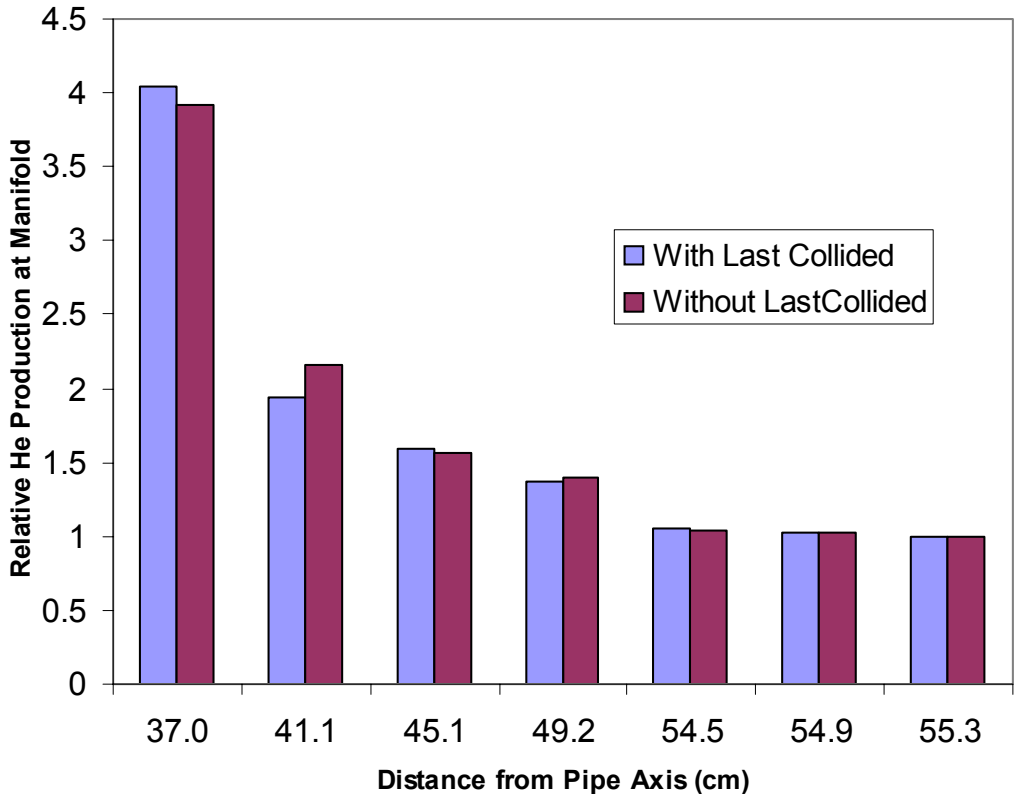

Figure A3. Helium production in manifolds with and without last collided option within 20-25 cm from pipe.

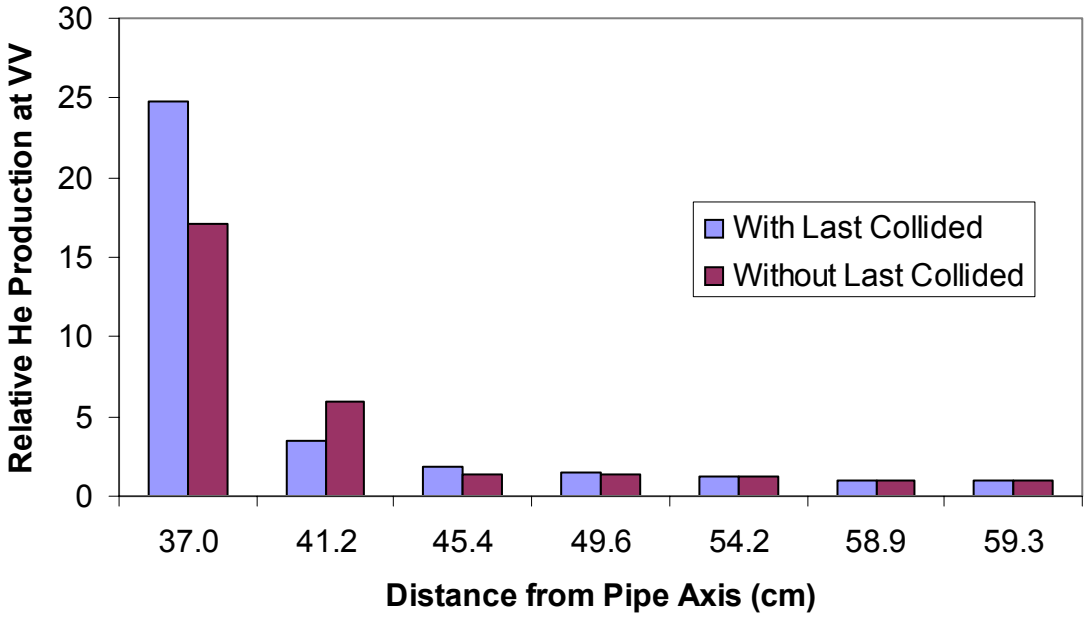

Figure A4. Helium production in vacuum vessel with and without last collided option within 20-25 cm from pipe.

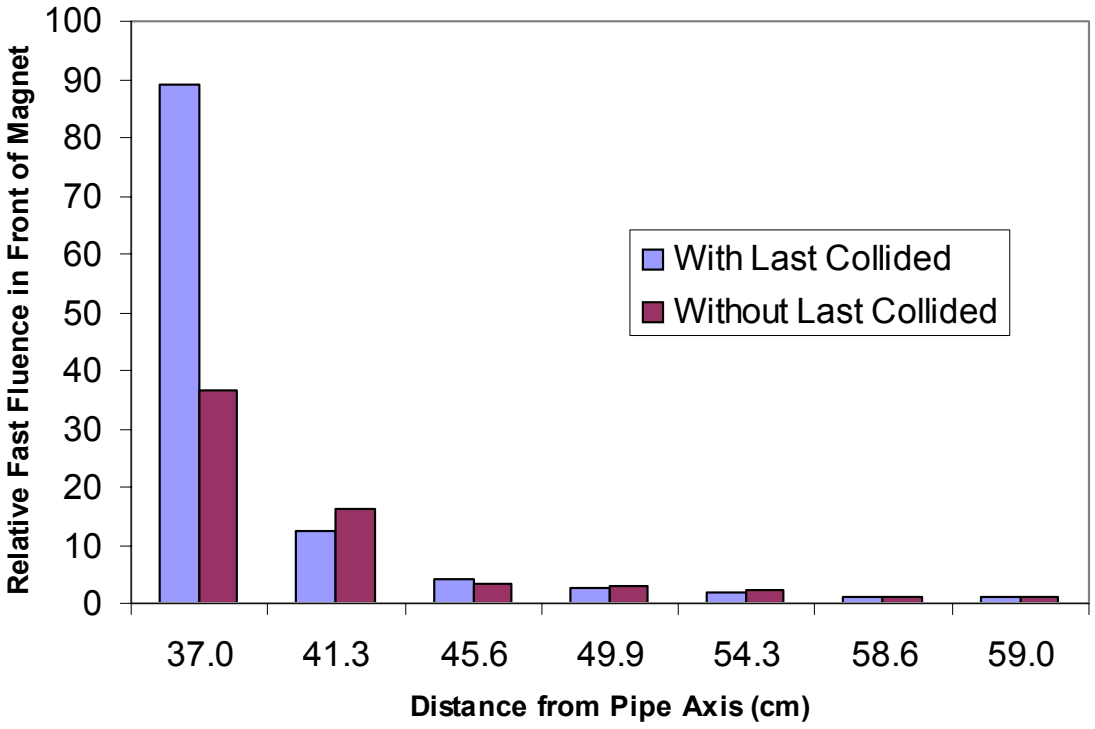

Figure A5. Fast fluence in front of magnet with and without last collided option within 20-25 cm from pipe.

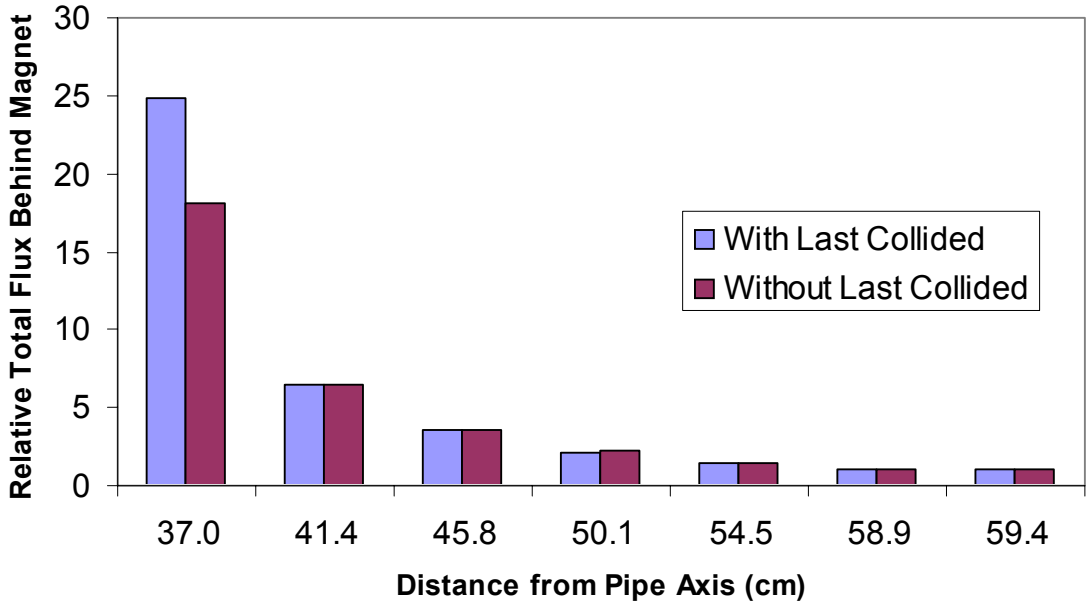

Figure A6. Total flux behind magnet with and without last collided option within 20-25 cm from pipe.

APPENDIX-B

Attila: Description, Options, and Nuances

Below we provide a brief description and outline some of the nuances and difficulties we have encountered with the Attila code during the neutronics analysis of the He pipe, divertor and torus only cases of the ARIES power plant. Some of the options are mentioned in the manual and others were uncovered after discussions with Transpire, Inc [3].

I. Brief Description of Attila

Attila is a finite element, 3-D discrete ordinates code for the solution of neutral particle transport. Major features of the code are:

- Discrete ordinates
- Multigroup energy format
- Legendre polynomial expansion of the cross section
- Accepts upscatter cross sections
- 3-D linear discontinuous finite element tetrahedral mesh
- Accepts CAD models from Pro-E, Cubit, etc. (use Parasolid files)
- Use of accurate integration quadrature sets: level symmetric, Gauss Legendre, etc.
- Will perform adjoint calculations
- Fixed source and alpha and k-eigenvalue problems can be solved
- First collided source option
- Last collided option
- Depletion calculation for reactor physics calculations
- Reaction rate – edit option

Transpire, Inc. [3] has completed their distributed memory and charged particle versions of the code.

II. Options and Nuances

1. Uncollided source options:

The Attila code has two uncollided source options and unfortunately one of them restricts the available boundary condition options.

- First Scattered Distributed Source (FSDS) option: this is a point source uncollided source option. It uses ray-tracing to obtain a distributed scattered source for further calculation. It works with reflective boundary conditions.
- S_n collision source option: this is a volumetric, uncollided source option. One can specify a high S_n order to obtain a good distributed scattered source for further calculation. It does not work with reflective boundary conditions. We also found out after following a rabbit trail that the albedo boundary condition does not work for this source option as well.
- Not quite an uncollided calculation: In principle, one can start a calculation with a high S_n order and stop the calculation after the 1^{st} group or a number of groups have converged. The high-energy flux would be computed with a high S_n precision. One

can restart the job using the scattered flux file (not sure of the name) and the lower energy groups would be run with a lower S_n order. See the restart option below for more details.

2. Boundary conditions:

The code allows for vacuum, reflective and albedo boundary conditions. However, there are restrictions on the use of reflective and albedo conditions:

- The vacuum condition can be used at any external boundary
- The reflective boundary condition can only be used on planes parallel to the x-y, y-z, and x-z planes. It cannot be used at arbitrary angles to the major planes
- There is an albedo option available for any external oriented surface. However, there are a few restrictions:
    - Though in principle the albedo should be energy dependent, the code will only allow one entry per surface. This means one value for all energy groups
    - The albedo implementation is a white condition (Transpire also calls it a diffusive condition). The radiation leaves at a given angle and is returned isotropically. For example, if the albedo is one, the number of particles leaving would be returning (net flow is zero), however, the specular reflection is not preserved.

3. S_n order:

There are restrictions on the highest S_n order that can be used in a calculation. For the Galerkin – Chebyshev quadrature set, the restriction is $n < 83$. Others also have limits. We were attempting a S_n first (or last) collided problem when we ran into this limit. Bias quadrature sets are also available.

4. Ray effects:

Ray effects will occur if one uses a low S_n order and transports a localized source into a large open distance space such as a point source with a large vacuum vessel surrounded by a blanket region or a small volumetric source that is surround by a large low scattering medium. Remedies are to use the uncollided source option or to increase the S_n order.

5. Last collided flux option:

There are instances where one would like to compute the flux at a point or at the end of a duct or pipe. The mesh may be large at this point or the resolution unsatisfactory. One can initiate a last collided flux calculation to compute the flux at this point. This works because the solution has converged in the surrounding mesh areas and the last collided flux option performs a numerical integration of the scattered source to that point.

- However, there is a quirk. If one uses this option to compute an edit or response (i.e. dpa or absorption rate) the code will redo the last collided flux calculation for each edit or response that is requested. This is a bug in the code; in theory, the flux should only be computed once. It can then be used to compute any number of responses.
- It is possible that the converged flux is negative and hence, a negative value will be integrated with positive values. One hopes the negative value does not dominate.

6. Mesh size:

At the moment there is no criterion to aid one's choice of a mesh size. This is a disadvantage. One must rely on experience and trial and error. One must rely on changing the S_n, P_ℓ, and model layering.

7. Layering:

Although in principle one can define any mesh size, in practice it is better to layer your regions in the direction of steep flux gradients. This forces smaller mesh dimensions in the direction of the gradient for better resolution and calculational performance (negative fluxes).

8. Coordinate transformation:

One can perform a coordinate transformation to have one of the major axes along the central axis of a pipe that is not initially aligned with one of the major axes for example. It turns out that certain quadrature sets have more points closer to the axis than in the middle of their range. This can be an advantage for certain type of problems.

9. Negative Fluxes:

Negative fluxes can appear in one's solution. These are unphysical values and are related to the numerical methods used in the code. For the traditional diamond difference discrete ordinates method in the 1-D case, there is a relationship between the mesh size, cross section value and lowest discrete ordinates angle (weight) that leads to a criterion for avoiding negative fluxes. One notes a similar interrelation between these three parameters for the Attila code. To avoid negative fluxes one typically changes either the mesh spacing or the S_n order because the cross section data is fixed as a property of the medium. If negative fluxes appear in non-important regions in your solution space, they may have little effect on the solution and may be ignored (but one should investigate). One can also use biased quadrature sets or rotate the axis to improve the solution in certain parts of the problem (see coordinate transformation).

10. Source input options:

One can input a flux guess as long as the mesh cell distribution aligns itself with the current mesh distribution (maps onto current mesh distribution). At the moment there is no boundary source or distributed source input option.

11. Reaction rate (edit) calculations:

Sometimes there is a need to perform reaction rate calculations using special cross sections and reaction parameters. The reaction rate or edit data can be part of the input library (working library) or is contained in a separate file (external file). Both of these options work well for a normal Attila run. However, one must create the external edit file based on a format provided by Transpire, Inc.

12. Reaction rate calculation using the last collided flux option:

The last collided flux option will only accept an external file for input of the reaction rate calculation. Unfortunately, for the calculation of multiple reaction rates, the current implementation in Attila will repeat the numerical angular integration for each reaction rate instead of performing a single integration to obtain the scalar flux, which can be used to calculate the various requested reaction rates. The way to get around this is to have the code compute the scalar flux and to do the reaction rate calculation external from the code within a spreadsheet or similar software. This can mean a lot of manual labor time spent to get the requested results.

13. Group collapsing:

Attila allows for internal group collapsing of a cross section library. The manual states that a single weighting function (flux) is defined for the entire problem and is used in every region for every isotope and material. At the moment it is not clear if the code will

accept multiple cross section sets to be used for different regions of a problem. We have not yet encountered this in the fusion area but it can be the case in a fission problem.

14. Memory usage:

An Attila calculation can be memory intensive. The memory usage depends on the S_n order, group structure, number of mesh cells and the P_ℓ order. A small utility code is provided that will allow a user to estimate the memory requirements for a calculation. If the entire job does not fit into RAM, then the low memory option is your next best option. It seems that only one group at a time is in RAM. This allows one to run a cell (mesh) intensive problem.

15. Restart option:

There is no true restart option. One can halt a job and the code will print out a moments file. This file can be read in as a flux guess to rerun (restart) the job. So in principle, the groups that have converged will only require one iteration and the calculation will proceed quickly to the group where the job was halted and will continue from there.

- However, this only works this way if vacuum boundary conditions have been applied. If albedo or reflective conditions are applied, the job begins anew as though for the first time and requires the same number of iterations in the groups that were converged as in the initial job. So no true restart
- The way to get around this is to cut the converged groups and just read in the flux moments for the remaining groups and then combine the results at the end of the calculation. Transpire, Inc. can be contacted for the details of this procedure. We currently do not have experience with this method.

16. Runtime:

The code runtime can be quite prohibitive for large mesh cell (hundred thousands of meshes) and S_n (n >16), and P_ℓ (ℓ>3) order problems.